

Wave Dynamics in the Stratosphere Revealed by Using GPS Radio Occultation (RO) Data

Toshitaka Tsuda

*Research Institute for Sustainable Humanosphere (RISH),
Kyoto University, Japan*

Collaborators

Simon Alexander, Andrew Klekociuk

Australian Antarctic Division, Australia

Yoshio Kawatani

*Japan Agency for Marine-Earth Science and Technology
(JAMSTEC), Japan*

Hayato Hei, Naoto Yoshida, Hiroo Hayashi

RISH, Kyoto University, Japan

Noersomadi

National Institute for Aeronautics and Space (LAPAN), Indonesia

M. Venkat Ratnam, Debashis Nash

National Atmosphere Research Laboratory (NARL), India.

OUTLINE

1. Introduction on atmospheric gravity wave and its role in maintaining the general circulation.
2. Characteristics of temperature profiles from GPS RO measurements, esp, its accuracy and height resolution.
3. Data analysis procedure of temperature perturbations (due to atmospheric waves) in the stratosphere using GPS RO data
4. Various generation sources of gravity waves
5. Global and regional behavior of gravity wave activities
 - ✓ Mid-latitude: jet stream, orographic generation (mountain waves), etc
 - ✓ Polar regions: polar vortex decay, orography and SSW (sudden stratospheric warming)
 - ✓ Equatorial region: tropical convection and effects of wave-mean flow interaction

Classification of atmospheric waves

(Middle atmosphere dynamics by D.G. Andrews, J.R. Holton and C.B. Leovy)

(1) Restoring mechanism

Planetary (Rossby) waves: Coriolis Effects (meridional potential vorticity gradient)

Gravity (buoyancy) waves: Gravity (stratification) (*)
(Inertio-gravity waves; combination of stratification and Coriolis effects)

(2) Forced waves

Forced waves are continually maintained by an excitation mechanism of given phase speed and wave number.

Thermal tides excited by diurnal solar heating

Free waves: gravity waves, normal modes

(3) Propagation

Some waves can propagate in all directions. But, horizontally propagating planetary waves can be trapped in the vertical under some circumstances

Equatorial waves can propagate vertically and zonally, but are trapped around the equator. Kelvin wave, mixed-Rossby-gravity (MRG) wave

(*) Typical scales of gravity waves

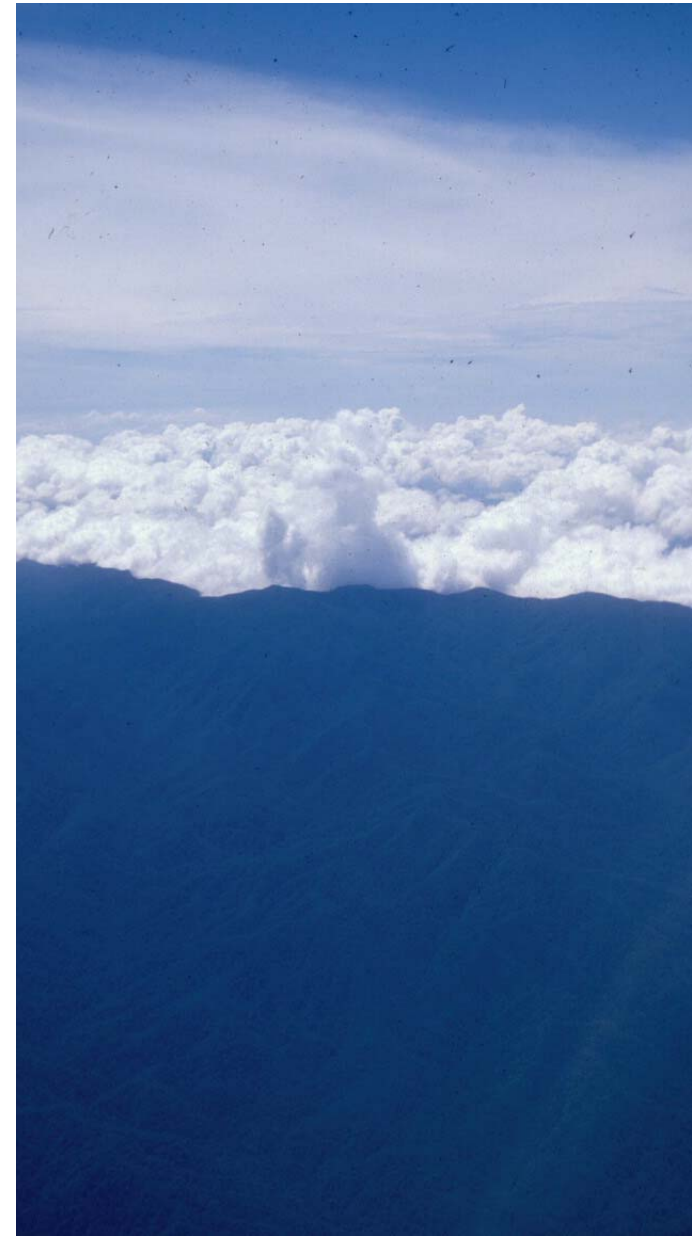
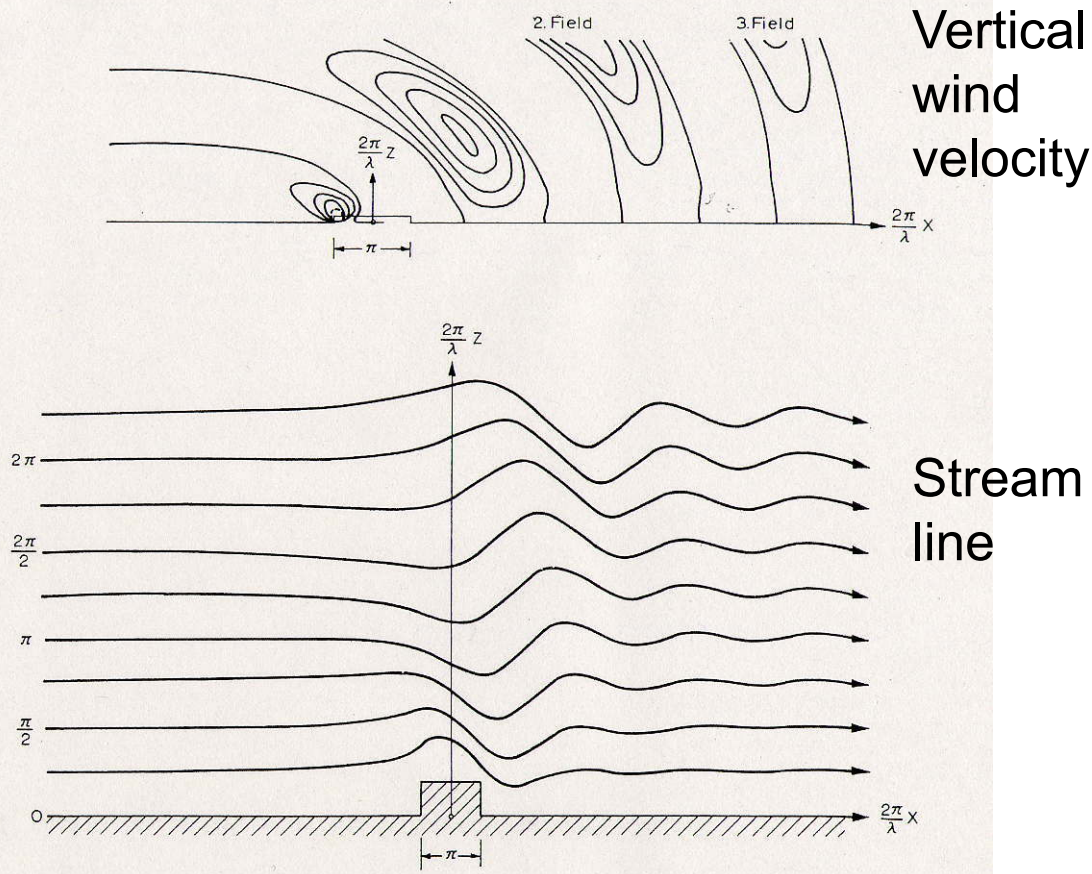
Wave periods: buoyancy (5-10 min.) to inertial (12hrs - several days) periods

Vertical wave length: shorter than 3-5 km

Horizontal scale: a few tens to thousands km

Excitation of atmospheric gravity waves

- Interaction of surface winds with topography (orographic, or mountain wave)
- Meteorological disturbances
- Jet stream
- Cloud convections in the tropics



(Gossard and Hooke, 1975)

Gravity wave generation by cloud convection in the tropics

Numerical model of gravity wave generation by tropical convection

T. Lane and M. Reeder (2001)

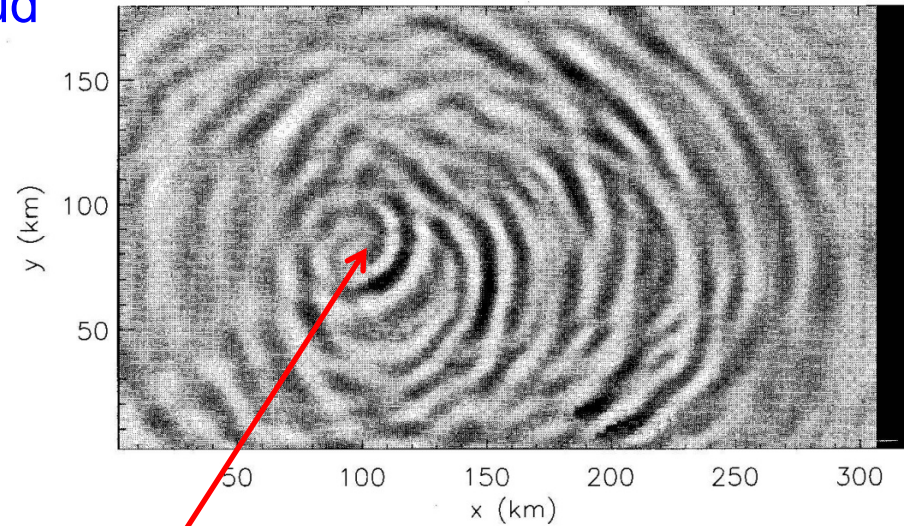


Figure 5. Horizontal cross-section of vertical velocity at $z = 40$ km in Domain 1 at 1330 LST.

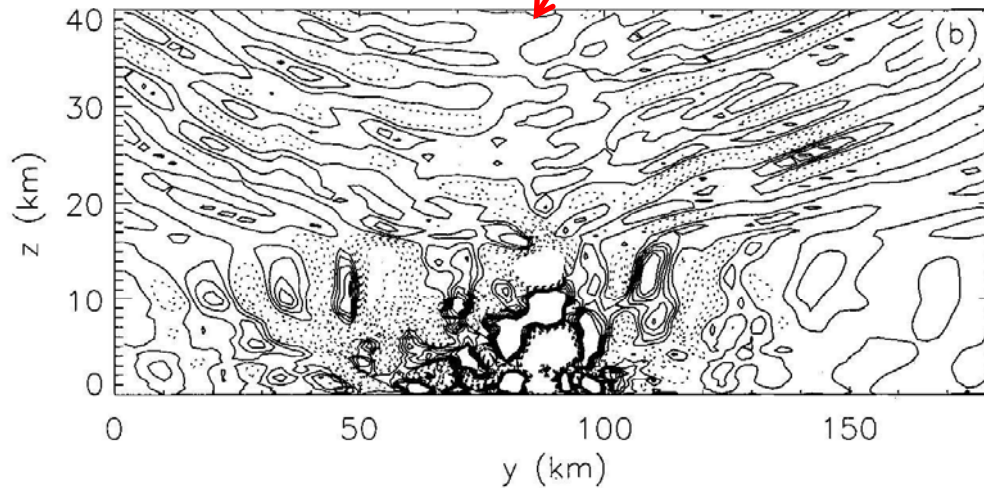


Figure 4. (a) Zonal cross-section of vertical velocity through $y = 100$ km for Domain 1. (b) Meridional cross-section of vertical velocity through $x = 100$ km for Domain 1. Vertical velocity is contoured at 0.1 m s^{-1} intervals, with the negative values dashed. Both plots are valid at 1300 LST. Note that (b) has a different horizontal scale from (a).



Convect
the North

Horizontal (top) and Height-meridional (left) cross section of vertical velocity

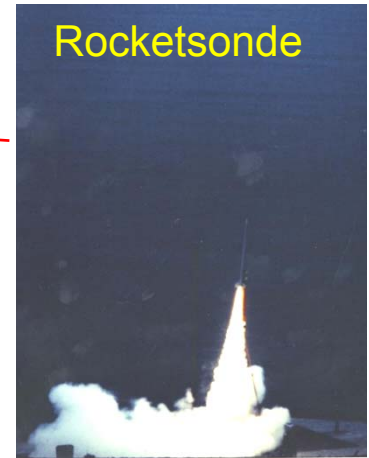
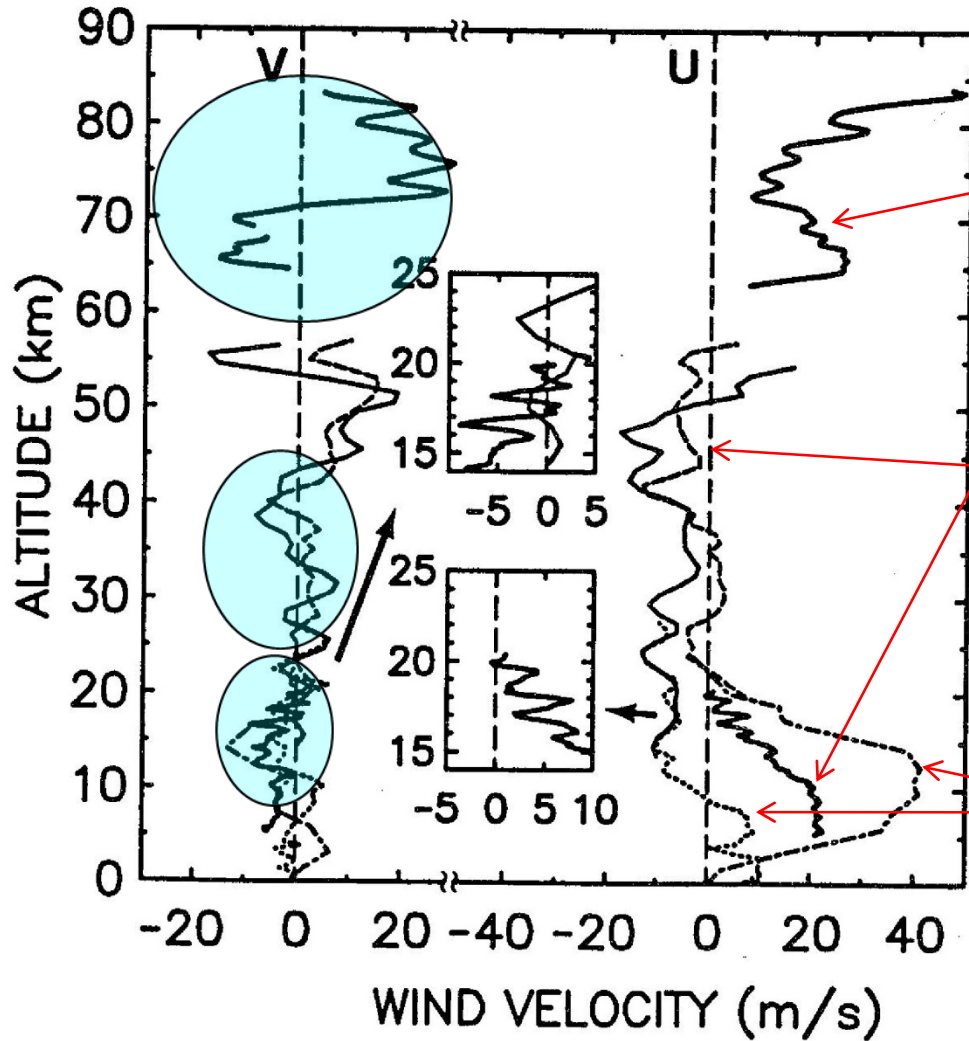
Typical wave parameters

$$\lambda_x \sim 15\text{-}20 \text{ km}$$

$$\lambda_z \sim 4\text{-}6 \text{ km}$$

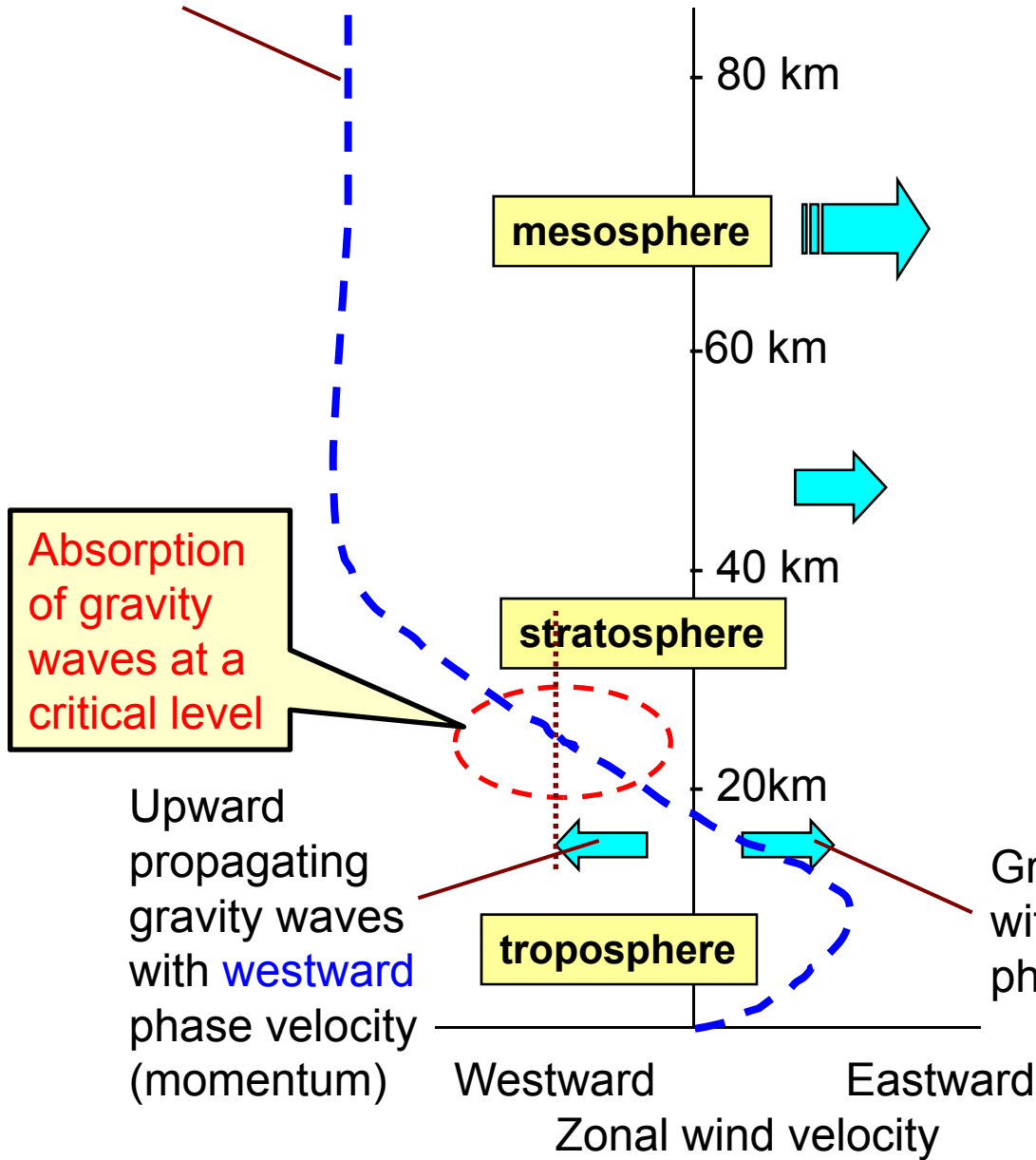
No preferential direction

Wind velocity profiles observed with the MU radar, radiosondes and rocketsondes



Both wave amplitudes and wave lengths (λ_z) increase along height.
 $\lambda_z = 2 - 3$ km in the lower stratosphere; $\lambda_z = 5$ km in the middle stratosphere;
 $\lambda_z = 10$ km in the mesosphere

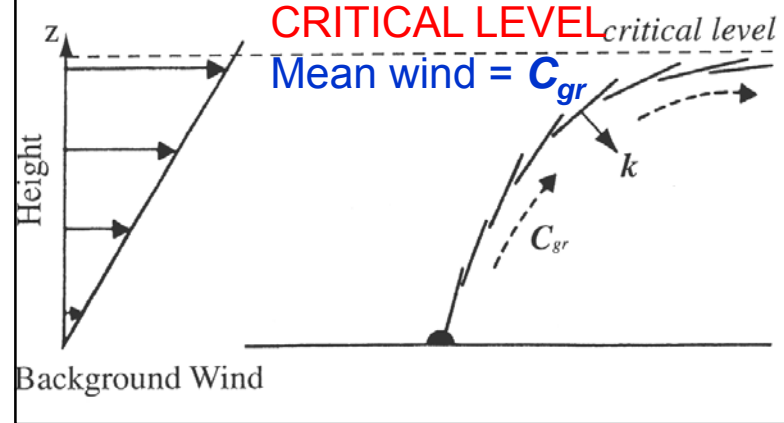
Mean zonal (eastward positive) wind velocity at mid-latitudes in the northern hemisphere
 Summer (assuming radiative equilibrium only)



CRITICAL LEVEL

Vertical propagation of a gravity wave in the vertical wind shear (LEFT). Short solid lines (RIGHT) show phase surface of the gravity wave [adapted from Matsuno and Shimazaki, 1981].

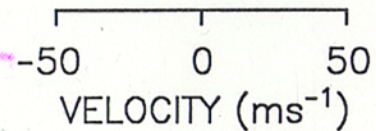
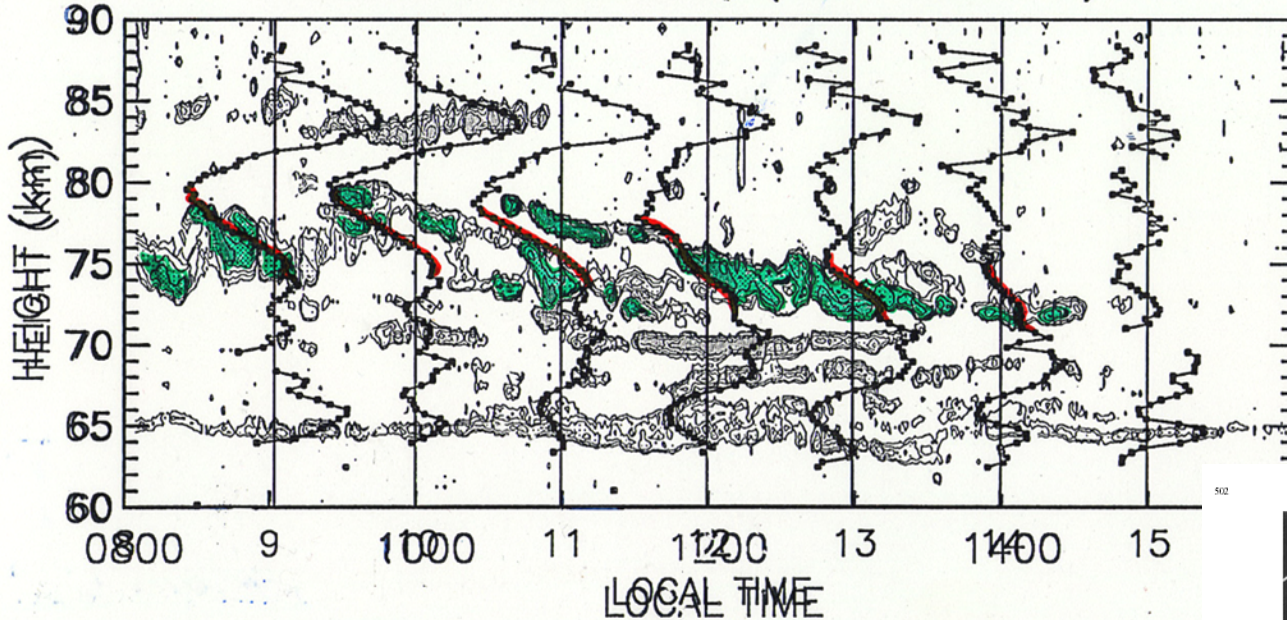
C_{gr} is the phase velocity of the wave. k is the vector perpendicular to the wave propagating direction.



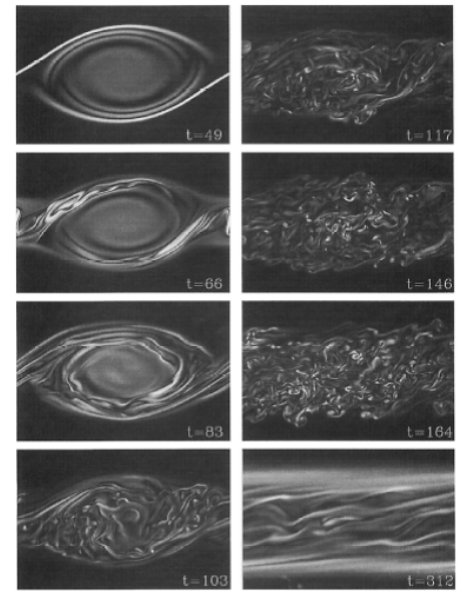
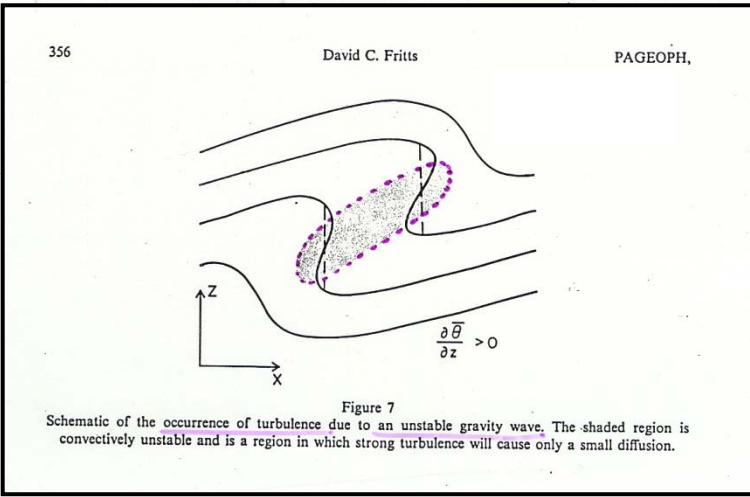
Radar Observations of Turbulence Echo Power (contour) and Hourly Meridional Wind Velocity



18 10 00 19 8 0 0 5 : 0 4 : 2 4 . 6 1 - 1 6 : 0 0 : 1 8 . 1 2
 EASTWARD COMPONENT (AZ = 0, ZE = 0)



Generation of turbulence due to breaking of gravity waves



502

R. J. HILL, et al.: TURBULENCE AND PMSE

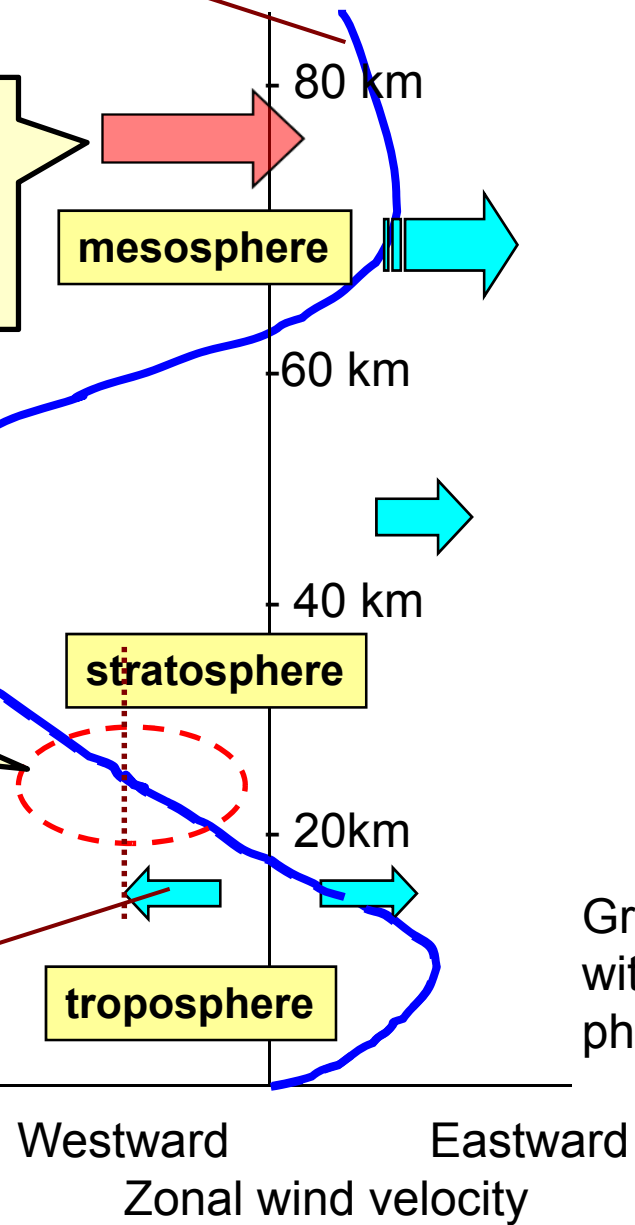
Fig. 1. Cross sections in a stratospheric vertical plane displaying the 3D evolution of vorticity magnitude. The 8 nondimensional times span the dynamical evolution, including early quasi-2D vortex roll-up ($t = 49$), transition to 3D structure consisting of stratospheric aligned convective rolls ($t = 66$ and 83), creation of a turbulent layer ($t \sim 83$ to 164), and eventual restratification and stabilization of the flow ($t > 200$).

Height Profile of Mean Zonal (eastward positive) Wind Velocity at mid-latitudes in the Northern Hemisphere Summer

Wave breaking by convective instability causes acceleration of background winds

Absorption of gravity waves at a critical level

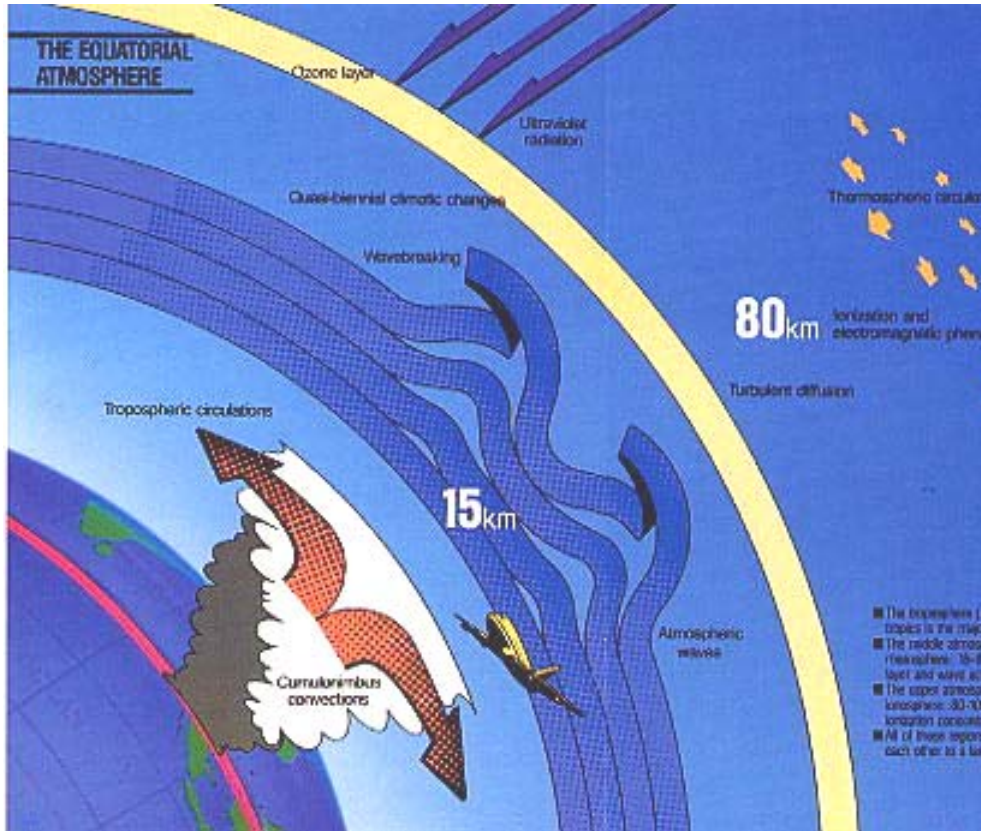
Upward propagating gravity waves with westward phase velocity (momentum)



CRITICAL LEVEL
 Vertical propagation of a gravity wave in the vertical wind shear (LEFT). Short solid lines (RIGHT) show phase surface of the gravity wave [adapted from Matsuno and Shimazaki, 1981].
 C_{gr} is the phase velocity of the wave. k is the vector perpendicular to the wave propagating direction.

Gravity waves with eastward phase velocity

Generation, Propagation and Dissipation of Atmospheric Gravity Waves (in the Equatorial Region)



(Dissipation)

The waves dissipate through various instability processes, and deposit the momentum to the background winds (acceleration), which plays a key role to maintain the general circulation of the atmosphere.



(Propagation)

These waves propagate upward, growing their amplitudes. The waves transport vertically the kinetic energy and momentum.



(Generation)

Active convection in the troposphere generates various atmospheric waves, such as gravity waves, equatorial Kelvin wave, etc.

AGU Chapman Conference on Atmospheric Gravity Waves and Their Effects on General Circulation and Climate (Hawaii, 28/2-4/3 2011)

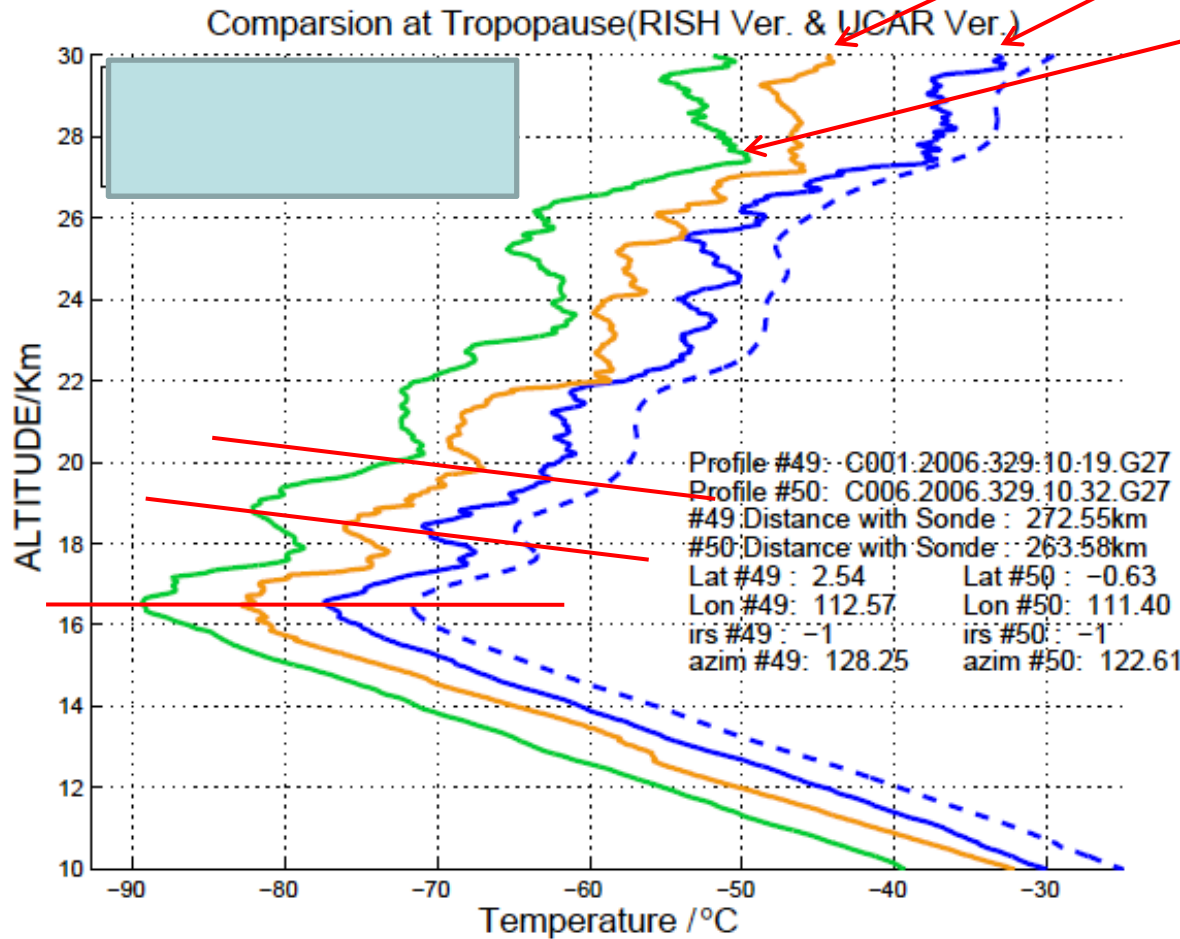
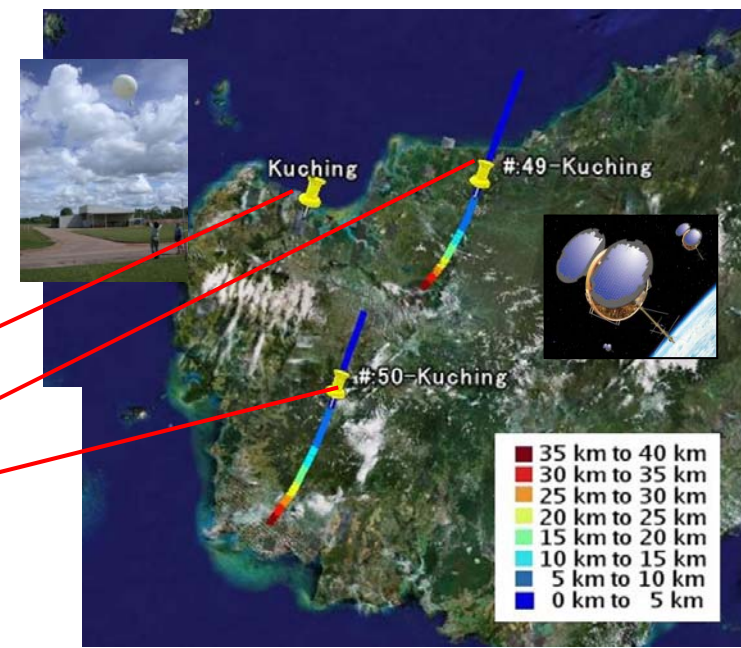
- Gravity waves are a dominant mode of variability in the atmosphere at **scales near the resolution** of current climate model simulations.
- They are generated by a variety of processes including the interaction of surface winds with **topography**, **deep convective storms**, and **unbalanced flow in the jet stream**.
- **Circulation changes associated with gravity wave dissipation** are now known to have wide-ranging effects on NWP, climate change response patterns, forecasts of stratospheric ozone recovery, and space weather.
- The global scale of these issues requires **global knowledge of gravity wave properties** despite the fact that **the scales of the waves themselves are too small to be fully simulated in a global model or fully sampled in global observations**.
- The problem of gravity waves and their effects on the general circulation thus requires a broad range of studies, those using **local high-resolution observations**, limited-area **wave-resolving models**, **global models**, and **global observational data sets such as those acquired from satellite**.

The GPS RO data having a very good height resolution provides a unique opportunity to study a global morphology of stratospheric gravity waves.

2. Characteristics of Temperature profiles from GPS RO measurements. esp, height resolution.

Q: Is the small vertical scale temperature perturbation physically meaningful, i.e. manifestation of gravity waves, or just a measurement noise?

Comparison of temperature profiles between the two COSMIC GPS RO results (#49 and #50) and radiosonde at Kuching, Malaysia. Profiles are shifted by 5K each.



Temperature profiles with GPS RO have a height resolution comparable to a radiosonde.

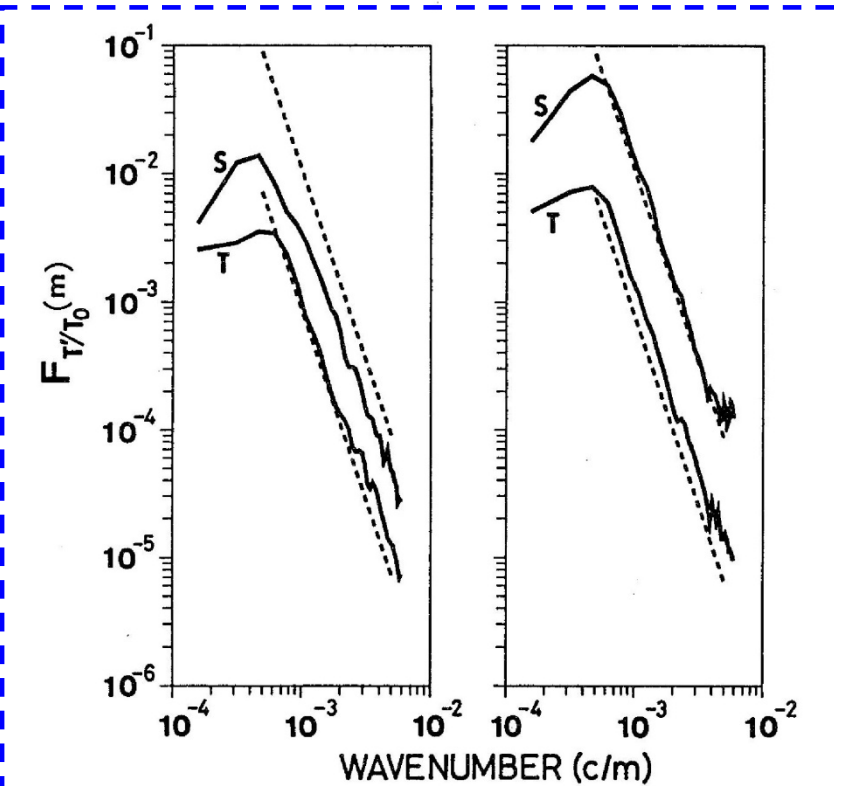
- detailed structure of the tropopause
- perturbations due to atmospheric waves

Vertical wave number spectra of temperature fluctuations (T'/T_0)

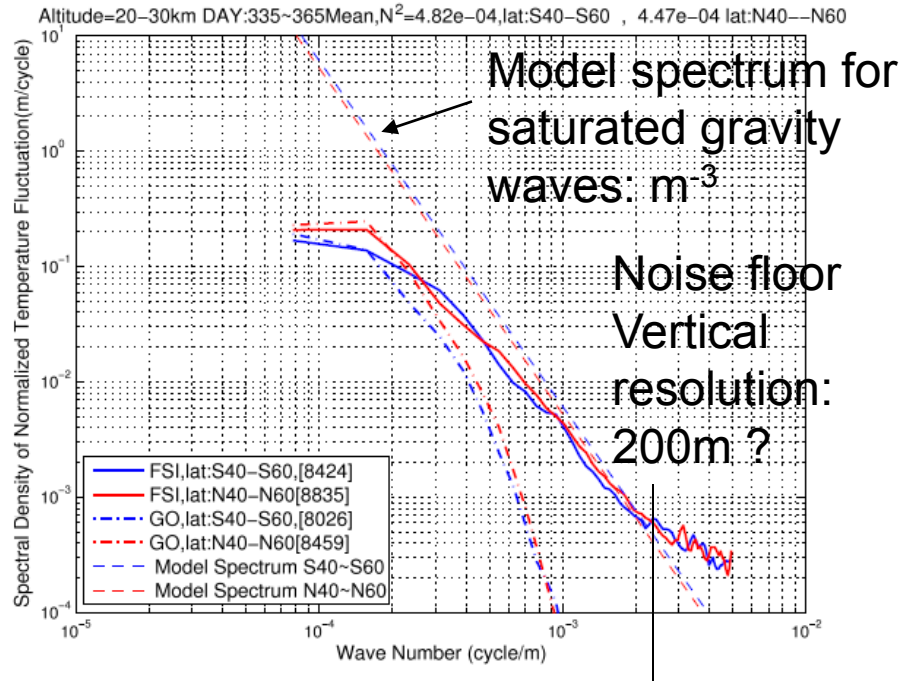
Gravity wave spectra from GPS/MET occultation observations, A.K. Steiner and G. Kirchengast, J. Tech, 2000

Vertical wave number spectrum of temperature fluctuations in the stratosphere using GPS occultation data, T. Tsuda and K. Hocke, J. Met. Soc. Japan, 2002

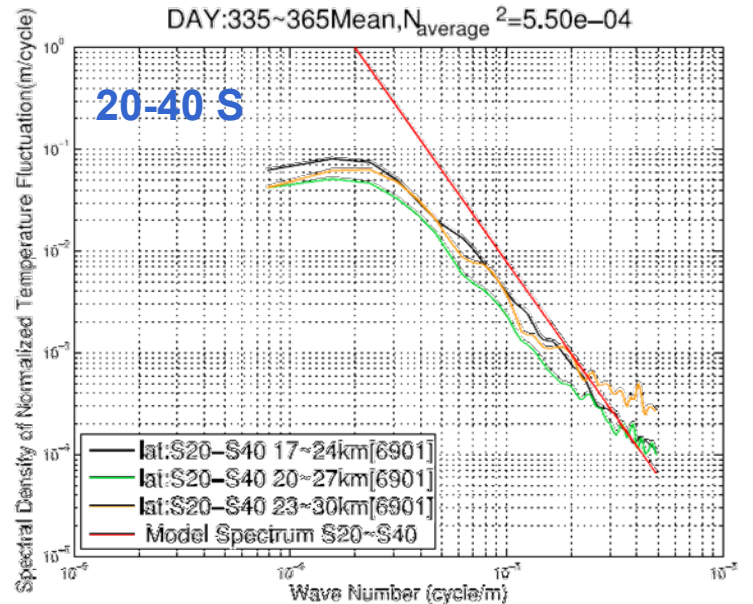
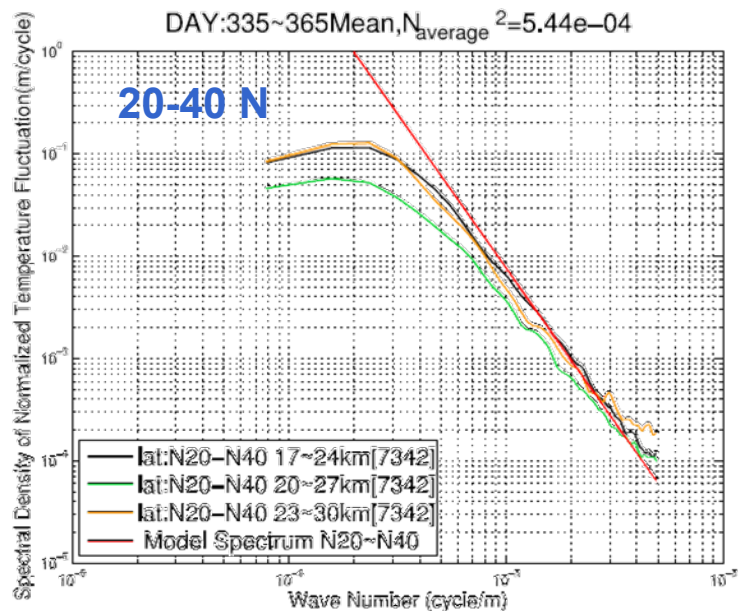
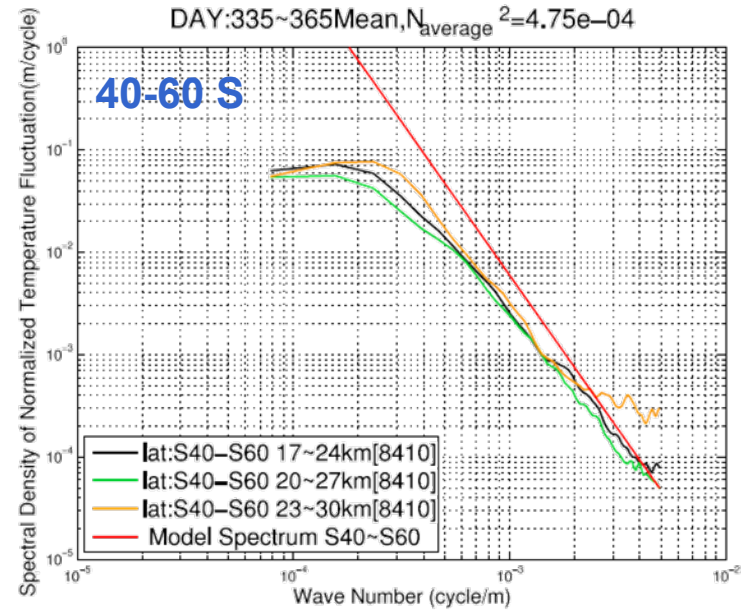
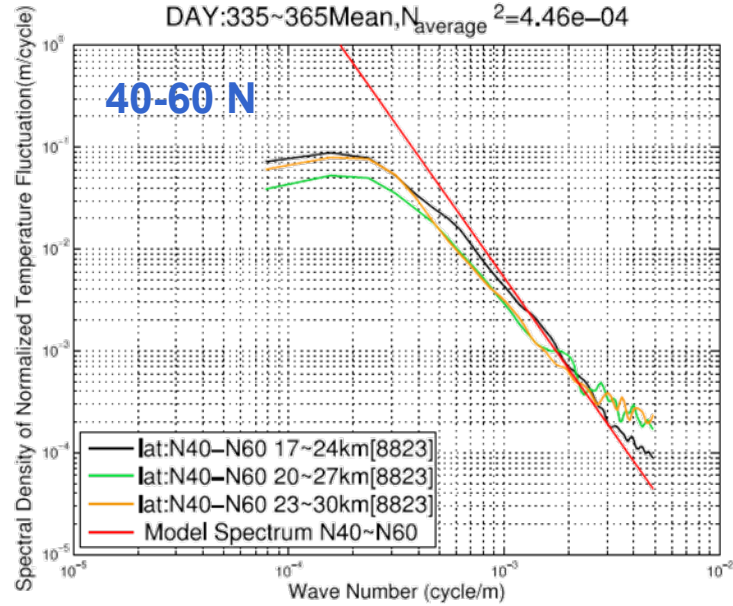
Spectra using GO (dotted line) and FSI (solid line) retrievals from COSMIC GPS RO data (40-60N and 40-60S)



Radiosonde results at 18.5-25km (S) and 2-8.5km (T) at the MU radar site, Japan, in summer (Left: Jun.-Sep. 1987) and winter (Right: Dec-Feb 1986/7) (Tsuda et al., 1991)



Vertical wave number spectra at 17-24 km (Blue), 20-27 km (Green) and 23-30 km (Red) in December 2006



3. Data analysis procedure of meso-scale temperature perturbations in the stratosphere using randomly distributed GPS RO profiles

Q: How can we separate T_0 and T' from GPS RO T profiles?

T_0 : mean profile in a longitude-latitude cell

T'_1 : sinusoidal fitting with zonal wave numbers

- Zonal propagation characteristics of equatorial waves, like Kelvin waves, MRG waves, planetary waves
- Mean profile for GW analysis (Wang and Alexander 2009)

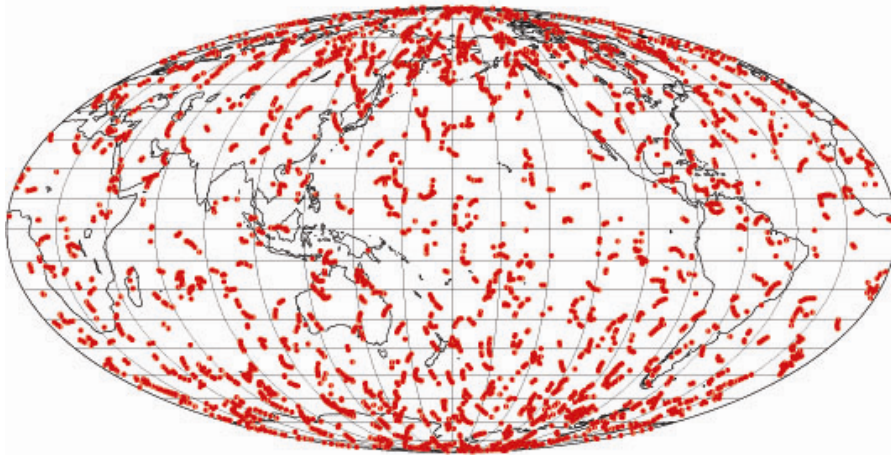
T'_2 : residual (Gravity waves)

- Gravity wave energy: temperature variance
- Spatial structure of gravity waves

Global Distribution of Gravity Waves with GPS RO Data

Climatological study (every 1-3 months) with CHAMP GPS RO data from May 2001- Dec 2005

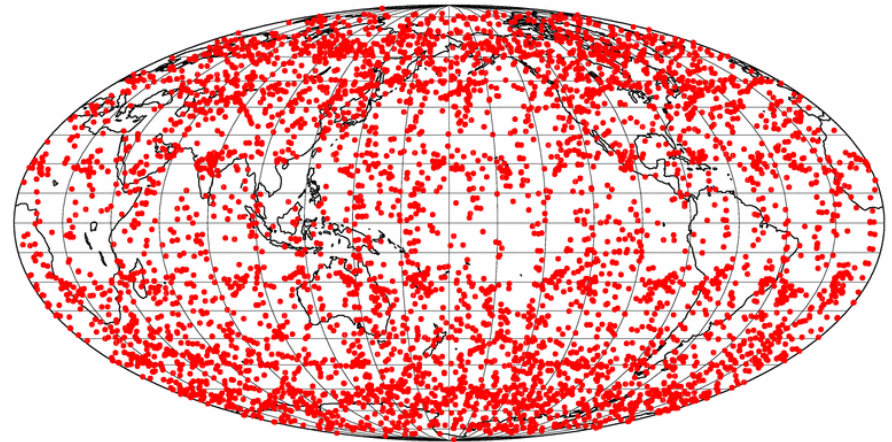
Distribution of the CHAMP GPS RO data in one month (October 2002)



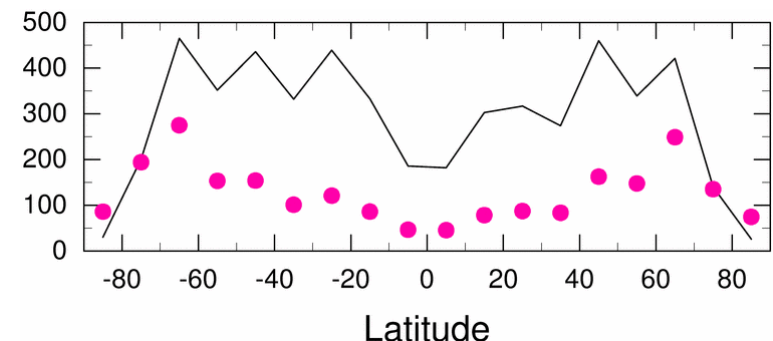
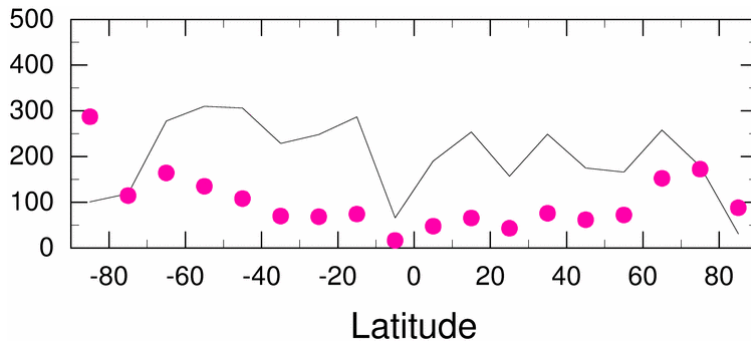
Analysis with COSMIC data after September 2006, with a time resolution of 5-10 days

COSMIC GPS RO data in 5 days on 18–22 September 2006

2006-09-18-2006-09-22



line: number of GPS data in each 10 deg, red dot: data rate normalized by the area

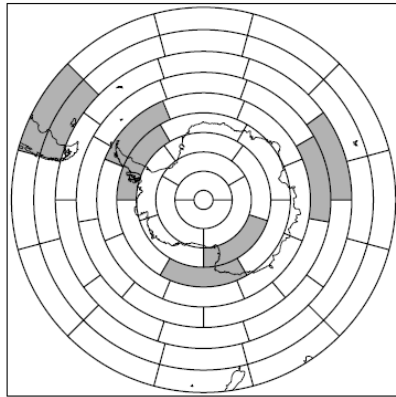


Atmospheric Gravity Wave Energy (PE or Ep) in the Stratosphere by Using GPS RO Temperature (T) Data

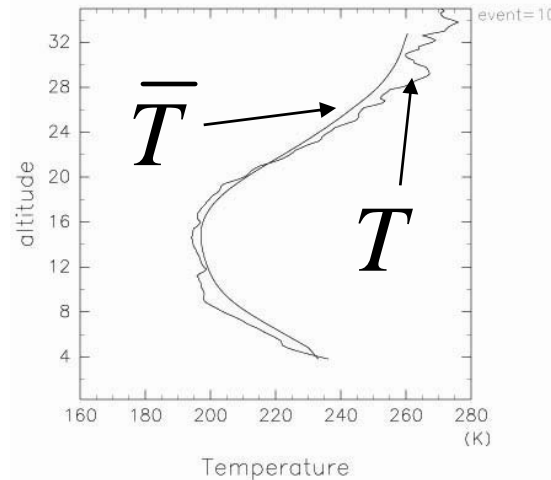
Wave potential energy, $PE=1/2(g/N)^2(T'/T_0)^2$

g ; acceleration of gravity, N ; Brunt-Vaisala frequency,

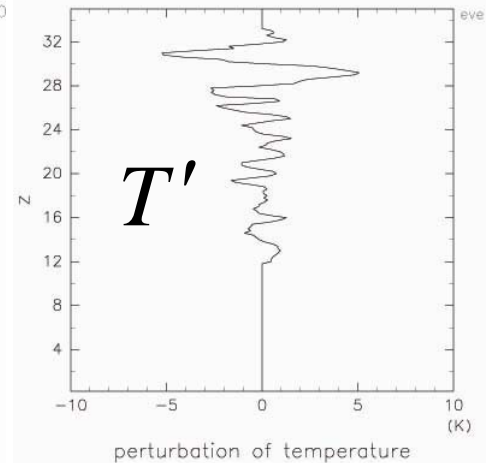
T' ; temperature perturbation, T_0 ; background temperature



temp+mtemp2003_Oct_event1013
(km)



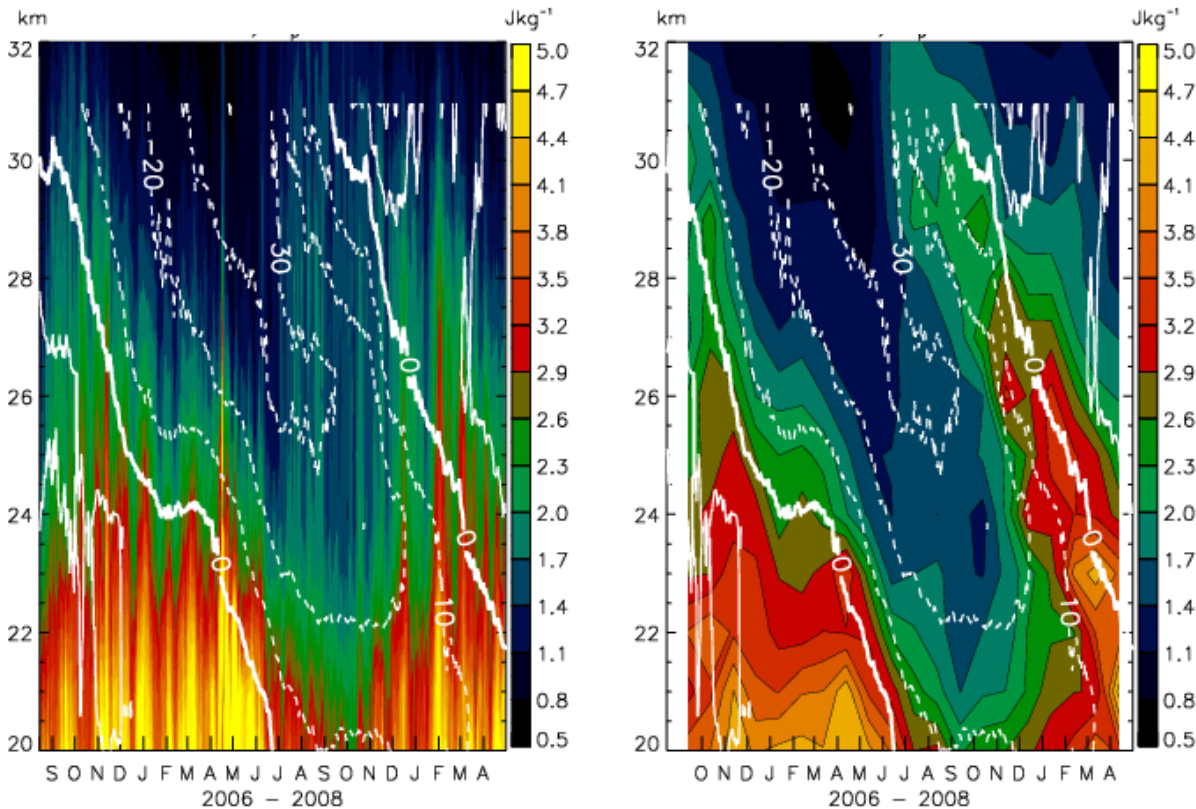
fcb_temp2003_Oct_event1013
(km)



Analysis procedure

- Select a time resolution: 5-7 days for COSMIC, one month for CHAMP
- Select longitude and latitude resolution of a cell : $20^\circ \times 10^\circ$, $10^\circ \times 5^\circ$
- Obtain mean T_0 :
 - Simple average of T in each cell and smoothing along height.
 - Decomposition into sinusoidal harmonics with zonal wave numbers.
- Extraction of T' : Calculate $T'=T-T_0$, then apply a high-pass filter with a cut-off at 5-10 km along altitude.

Season-height section of zonal mean PE at 25.S-2.5N from Sep 2006 to Apr 2008



- QBO westward shear initially, then eastward shear after mid-2007.
- QBO removes gravity waves, especially close to the 0 m/s phase line.

LEFT:

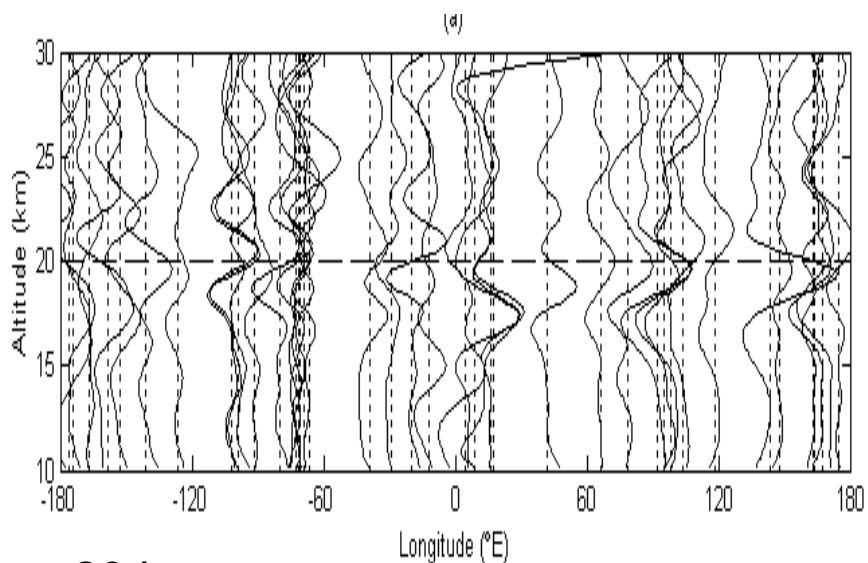
- Grid size: $20^\circ \times 5^\circ \times 7$ days,
- 7km high-passed perturbations from individual profiles, and get PE by integrating vertically over 7km, stepping up by 1km and forward by 1 day.
- Mainly meso-scale GWs with minor MRGW and higher speed KW contributions.

RIGHT

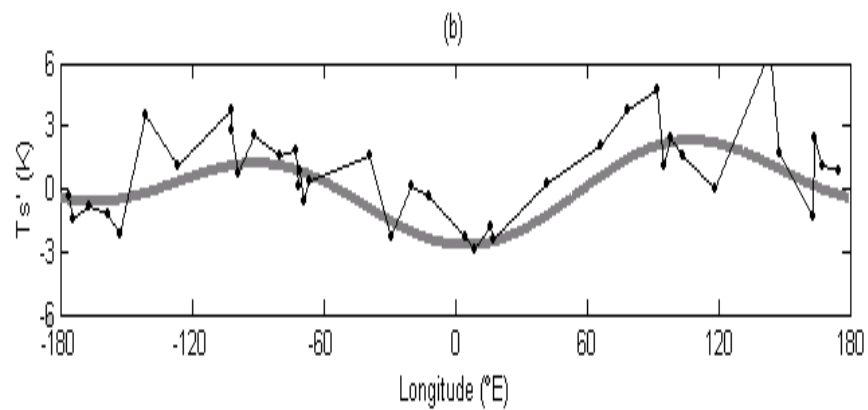
- Grid size: $20^\circ \times 5^\circ \times$ one month
- Height independent (1km) data by assuming that all wave phases are represented at that particular height
- Slower speed KWs but still mainly consists of GWs

White contours: NCEP zonal mean zonal wind, units m/s, east/westward; solid dashed

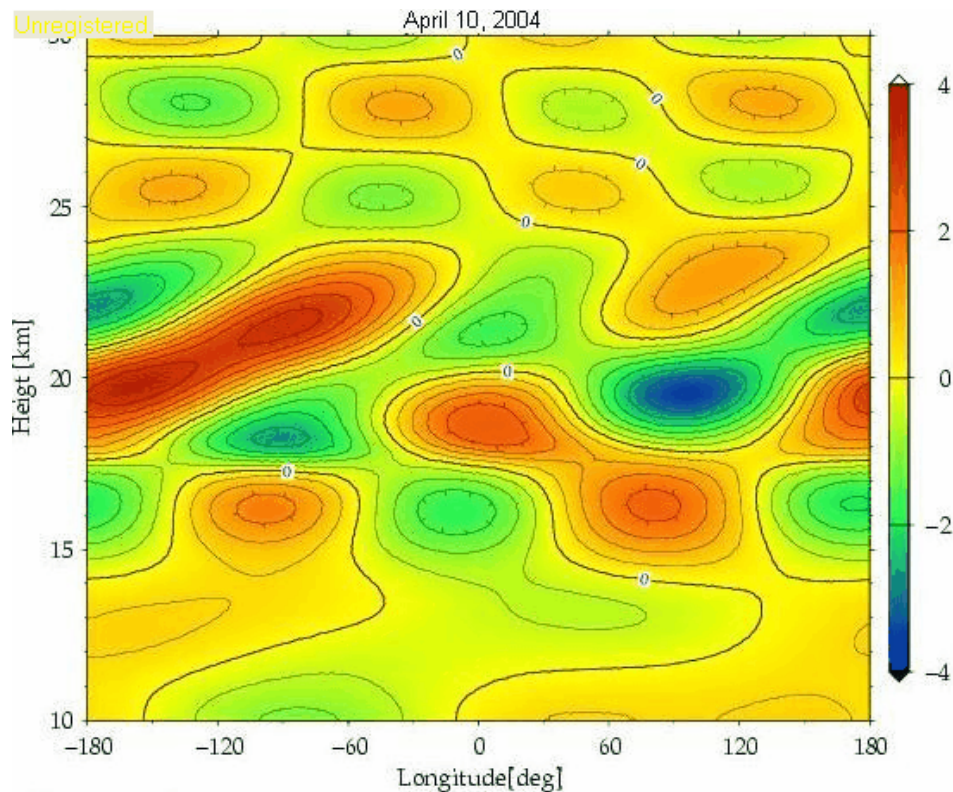
Residual temperature fluctuations (T') at 10°N - 10°S , and longitude variations of T' at 20 km altitude during 3-5 May 2004.



20 km

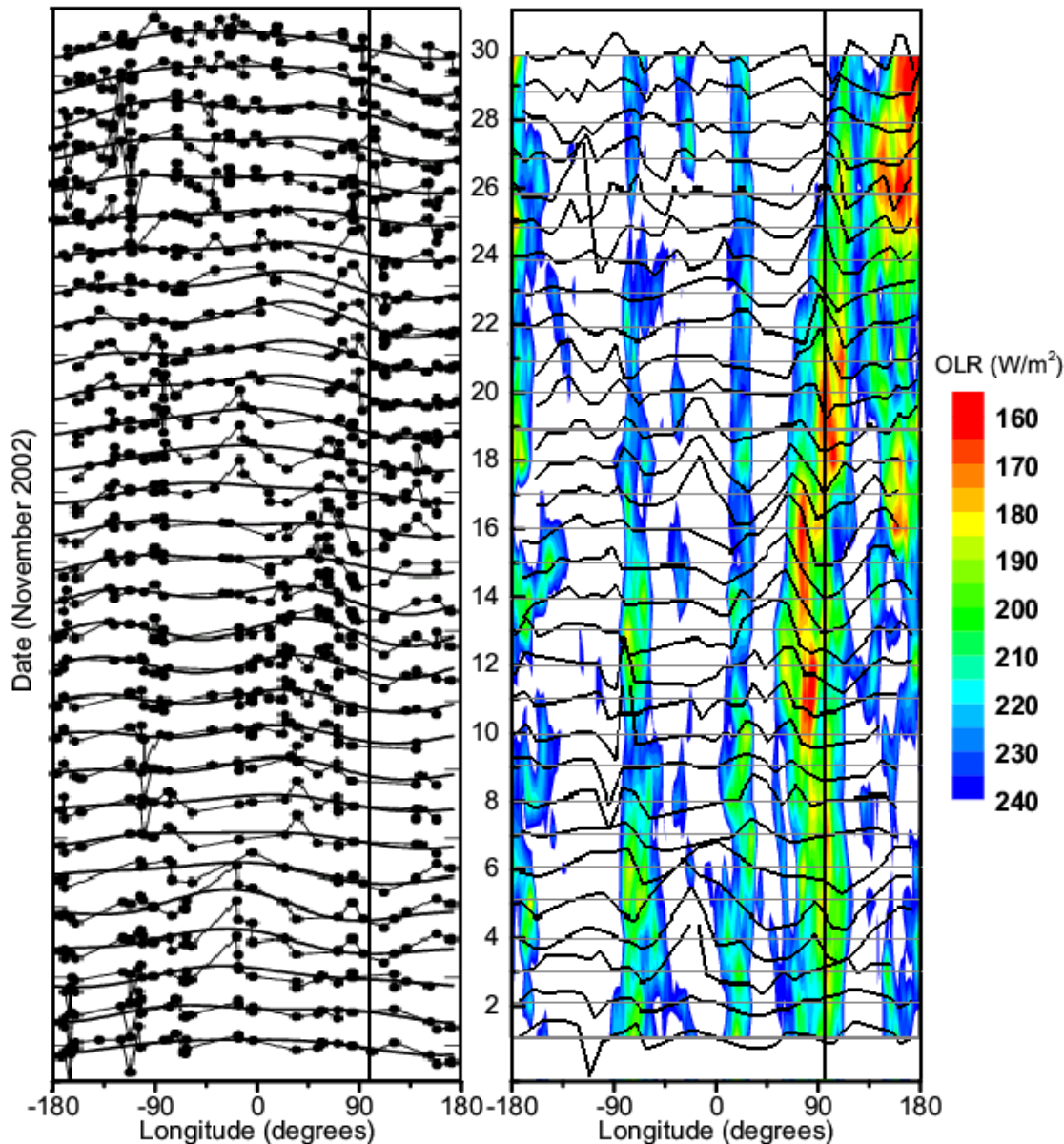


Longitude-Height variation of Kelvin waves in April-May 2004 (CHAMP)



Kelvin wave-like perturbations with zonal wave numbers 3-4 during enhanced cloud convection in the tropics (Ratnam et al., 2006)

CHAMP



(left panel)

Time-longitude variations of T' (dotted thin line) and TF' (smoothed curve) at 16 km in November 2002.

T' and TF' are constructed every three adjacent days and are vertically shifted to the middle date daily. Each curve is shifted 4 K vertically. The vertical line at 100E.

(right panel)

Time-longitude section of OLR over 10N-10S (contour)
Time-longitude variations of the deviation from the TF' ($TF' - T' = TR'$) at 16 km.

Horizontal structure of gravity waves from series of GPS RO profiles

Spatial structures and statistics of atmospheric gravity waves derived using a heuristic vertical cross-section extraction from COSMIC GPS radio occultation data

Takeshi Horinouchi and Toshitaka Tsuda
(JGR, doi:10.1029/2008JD011068, 2009)

- During early stage of COSMIC, multiple LEO satellites successively passed over the same orbit, resulting in quasi-linearly aligned GPS RO profiles with separation of 1,500-5,000 km. Then, almost instantaneous (within 1 hr) snapshots of vertical-horizontal cross sections of atmospheric temperature could be obtained.
- Horizontal wavelengths of GWs in the winter (here northern) hemisphere were generally smaller than those in the equatorial region or in the other hemisphere.
- For GWs in the northern mid-latitudes, both eastward and westward propagations relative to background winds were identified. The GW amplitude had a negative correlation with zonal wind shear. In the meridional direction, northward propagation was dominant, indicating that the dominant source region of meridionally propagating GWs was in the subtropics.

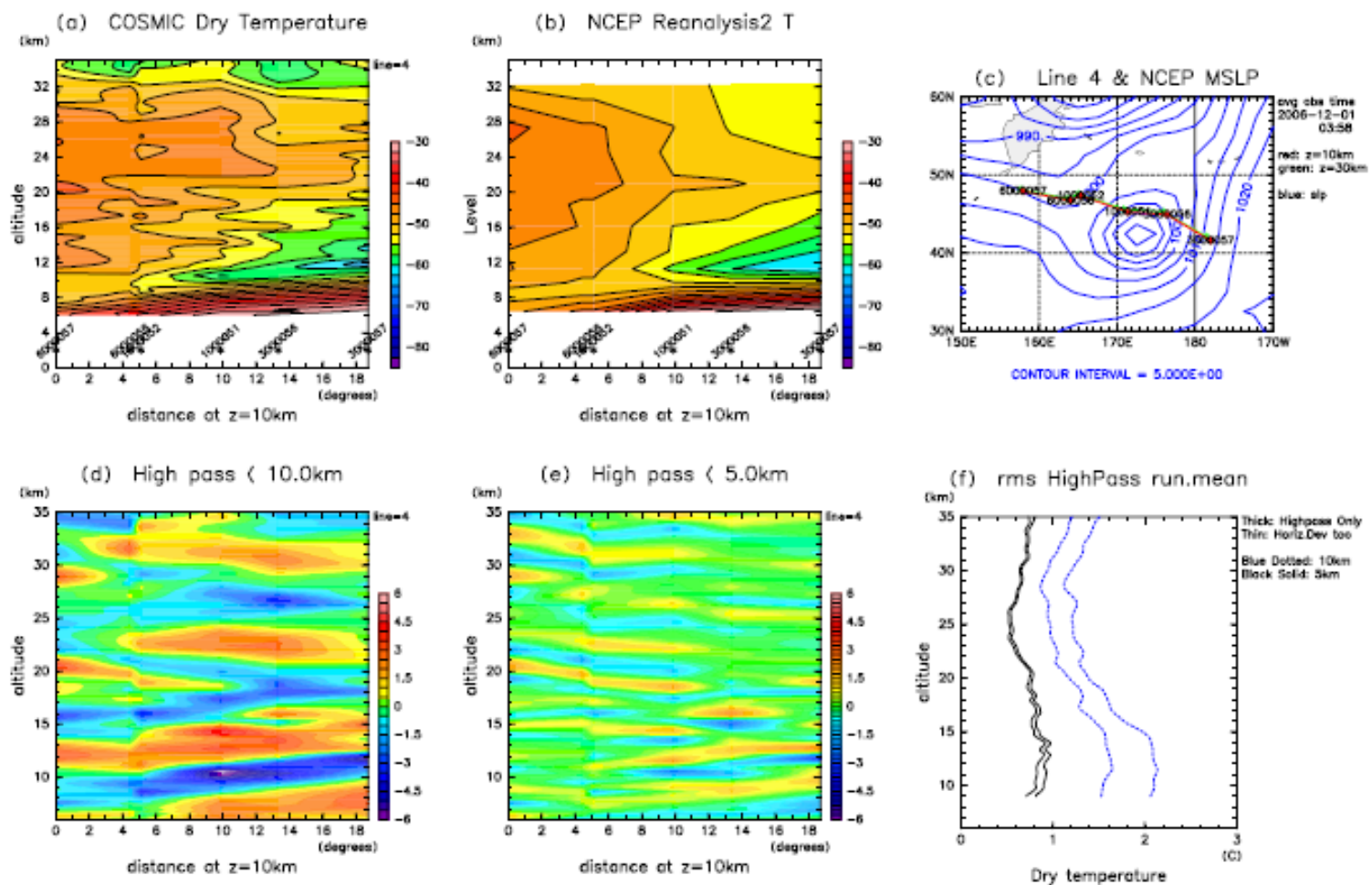
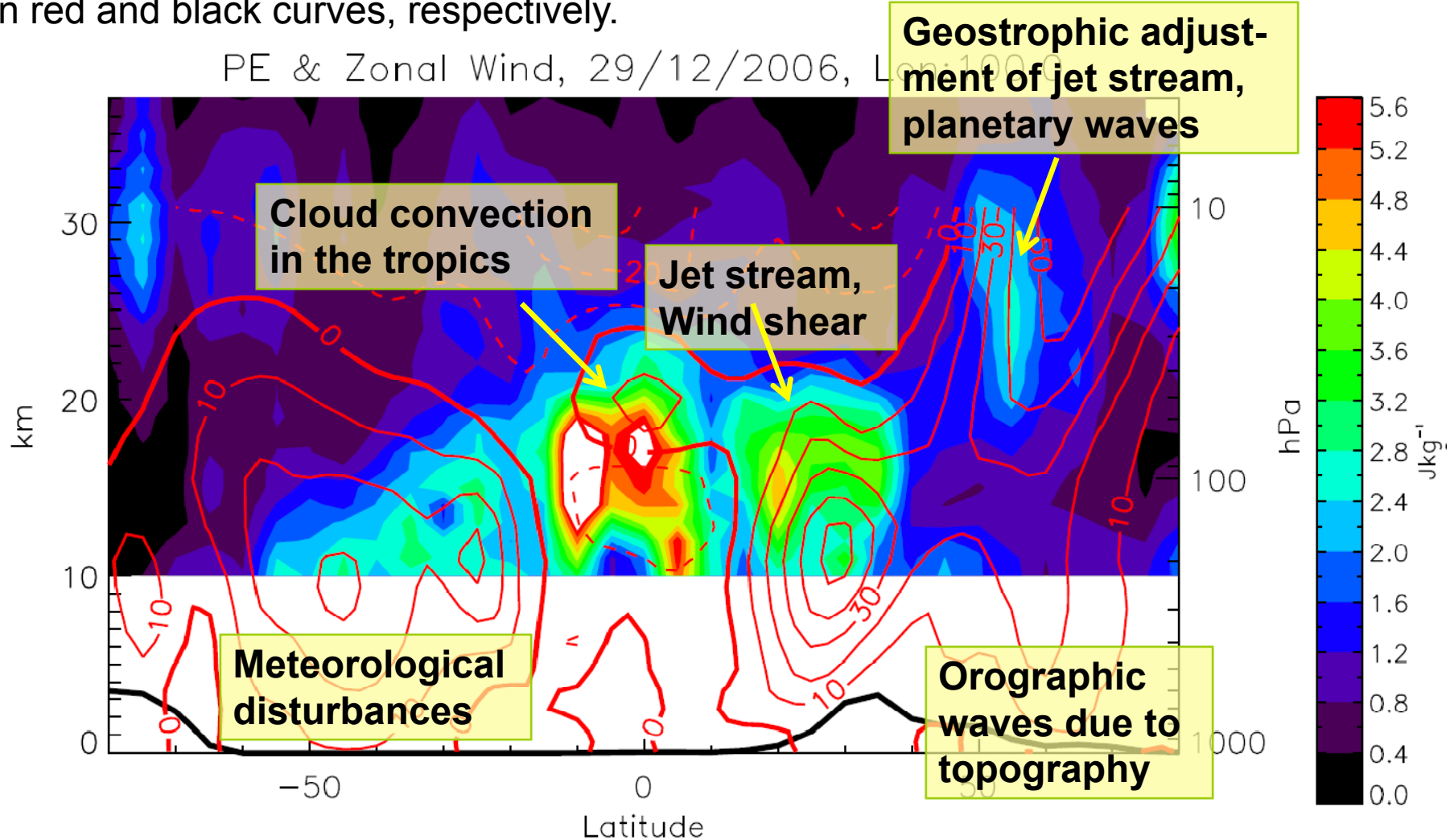


Figure 6. (a) Vertical cross section of the dry temperature along a line obtained on 1 December 2006. (b) The temperature from the NCEP reanalysis 2 data sampled at the same data points after linear interpolation. (c) The locations of the data points, where the tangent points at the altitude of 10 km are shown in red and those on top of the tangent points at 30 km, which are almost hidden, are shown in green. The times of occultations are shown in the right margin of Figure 6c. The blue contours show the sea level pressure from the NCEP data. Horizontal axes of Figures 6a, 6b, 6d, and 6e are the locations of the tangent points at 10 km projected onto the line segment between the two ends of the line with the westernmost point on the left-hand side. Figure 6c shows the temperature from the NCEP reanalysis 2 data interpolated horizontally to the data points. COSMIC dry temperature disturbances obtained by the high-pass filtering with (d) $\lambda_{zc} = 10$ and (e) $\lambda_{zc} = 5$ km. (f) The root-mean-square amplitudes with running means for $\lambda_{zc} = 10$ and 5 km in blue and black, respectively, and without and with the subtraction of horizontal averages (see section 4.1) with thick and thin lines, respectively.

4. Various Generation Sources of Gravity Waves

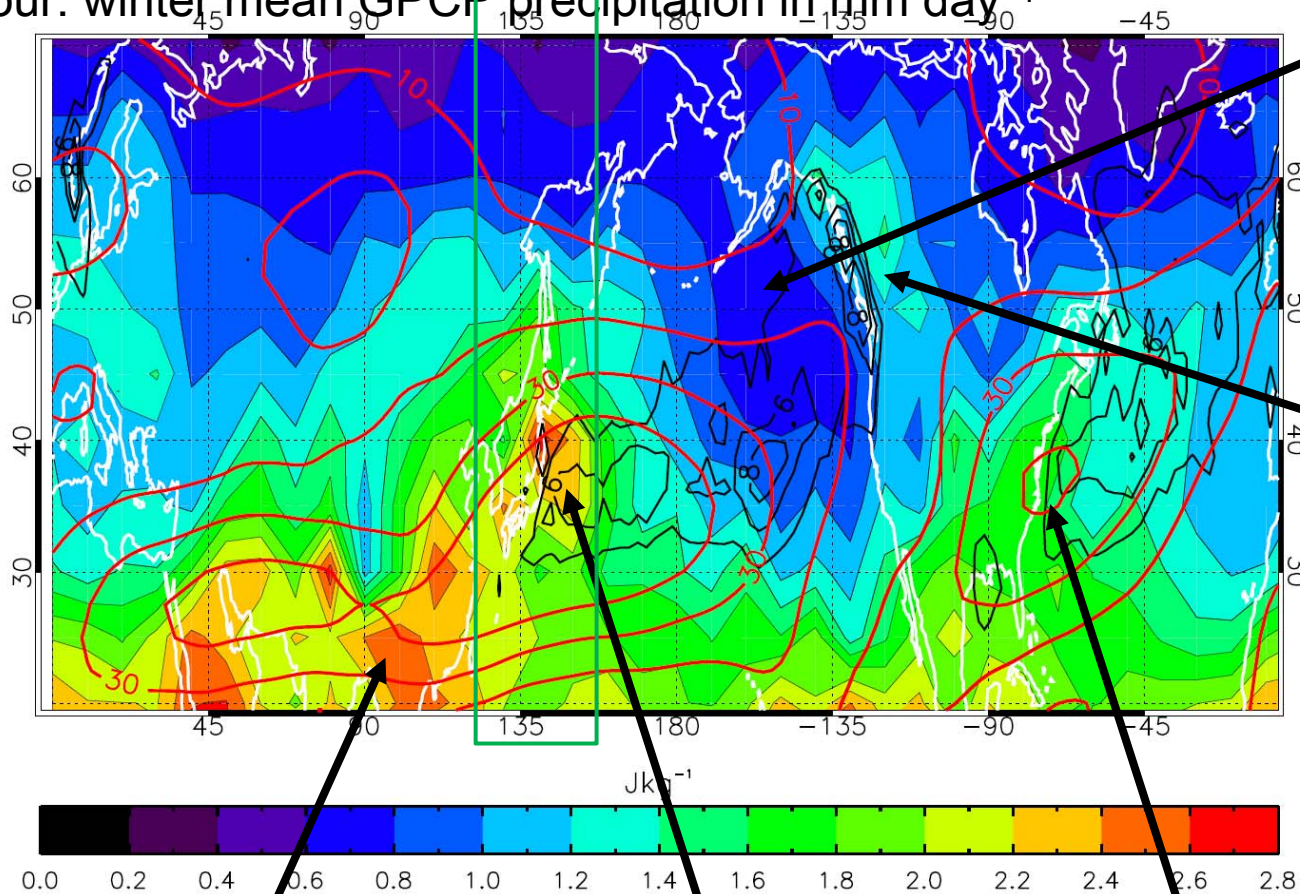
A height-latitude section of the wave potential energy (E_p) (T' with vertical wave lengths < 7 km) from the COSMIC GPS RO data in 7 days centered on **December 29, 2006 at the longitude of 140°E ($130^\circ\text{-}150^\circ\text{E}$)**. Zonal winds from NCEP and topography (elevation) at 140°E are also plotted in red and black curves, respectively.



Gravity wave potential energy (E_p) at 17–23 km altitude in winter 2006/07 (Dec-Feb) by using the COSMIC GPS RO temperature data.

Red contour: the winter mean NCEP u at 500–100 hPa in units of ms^{-1} .

Black contour: winter mean GPCP precipitation in mm day^{-1}



Ep is low over Pacific

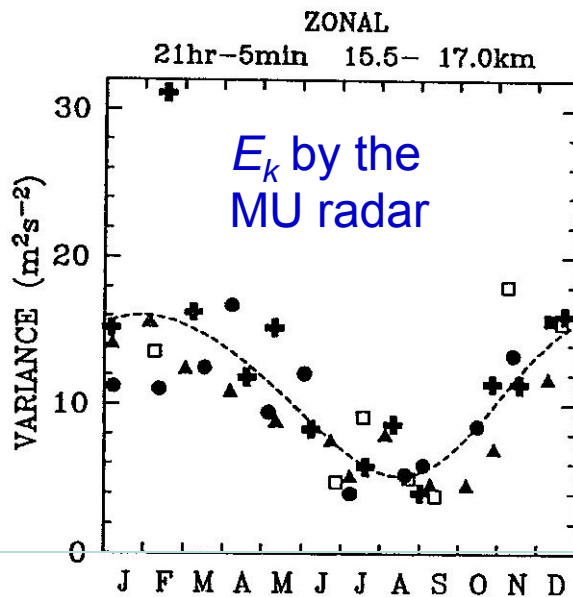
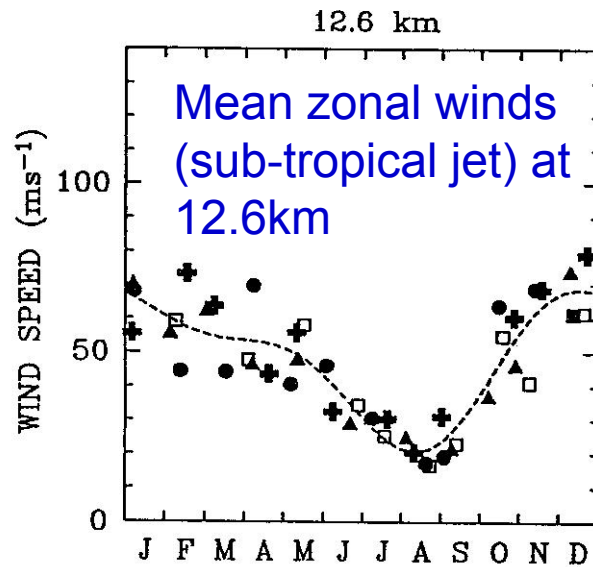
Canadian Rockies have large Ep

Himalayas & Tibet have large Ep – some orographic effects but also jet stream

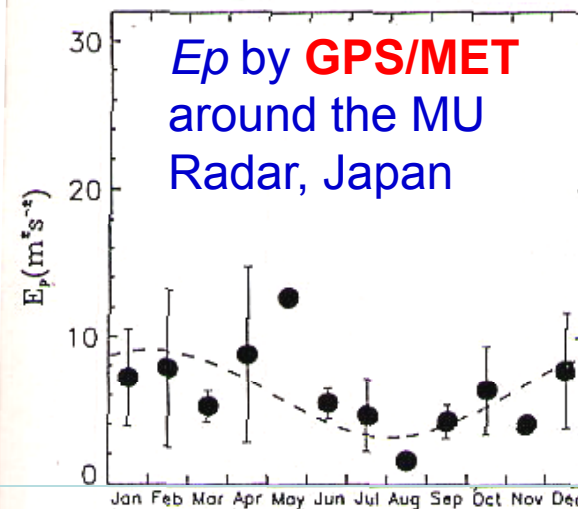
Japan – separate large Ep: strong jet & orography

Large Eastern USA Ep associated with strong winter jet

Comparison of GW energy between ground-based radar (MU radar) and GPS RO data (GPS/MET)

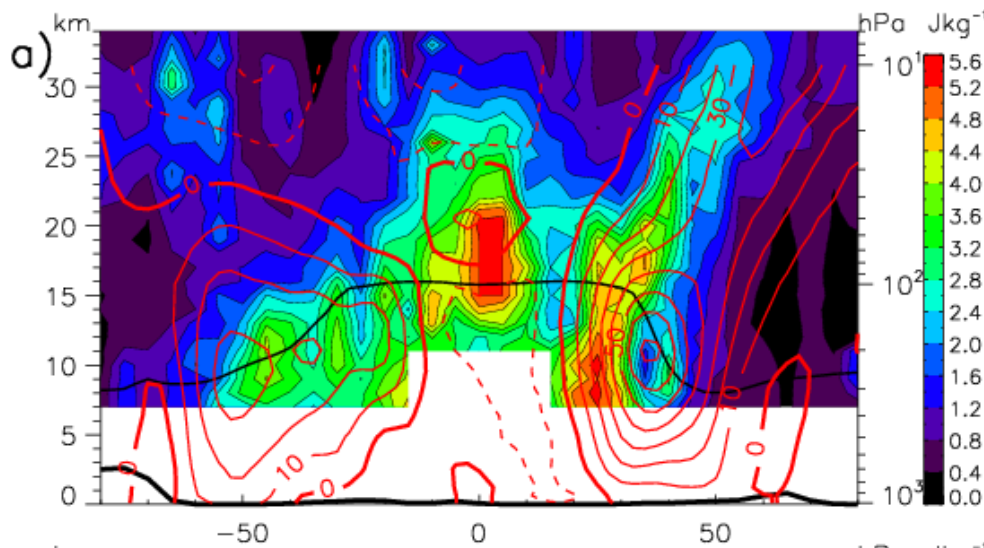


1. Monthly mean E_p
 $= \frac{1}{2}(g/N)^2(T'/T)^2$ at 15-20 km around the MU radar, Japan (35°N, 136°E) in 1985-1989.
2. Seasonal variations of E_p from GPS/MET agree well with the climatological behavior of E_k (wind velocity variance) due to gravity waves observed with the MU.
3. $E_k/E_p = 1.67-2.0$
 Theoretical prediction = 1.7.



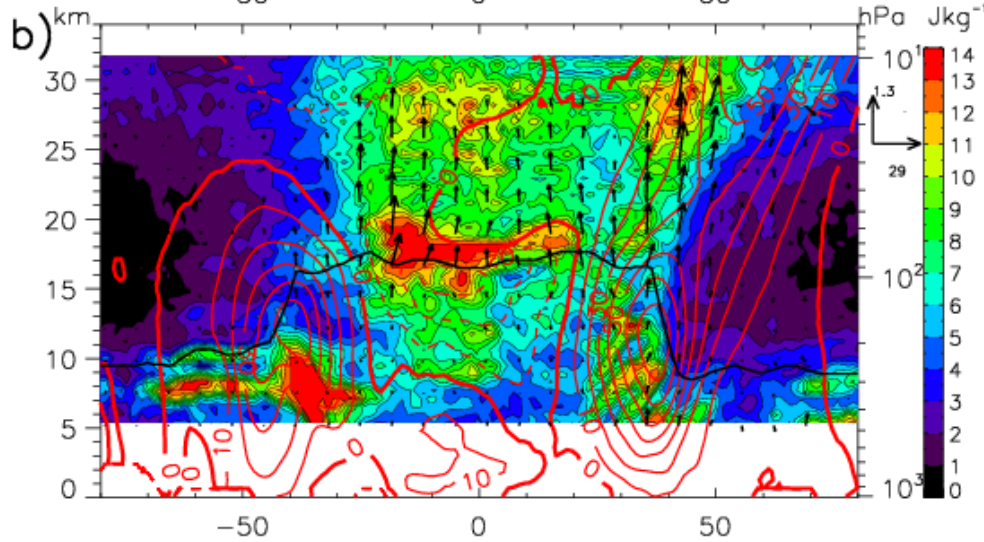
Generation of gravity waves by polar vortex decay and orographic effects in the polar regions





COSMIC PE at 140E during 12 – 18 Dec 2006

- Strong winter time sub-tropical jet
- Large PE from mid-troposphere up to polar night jet



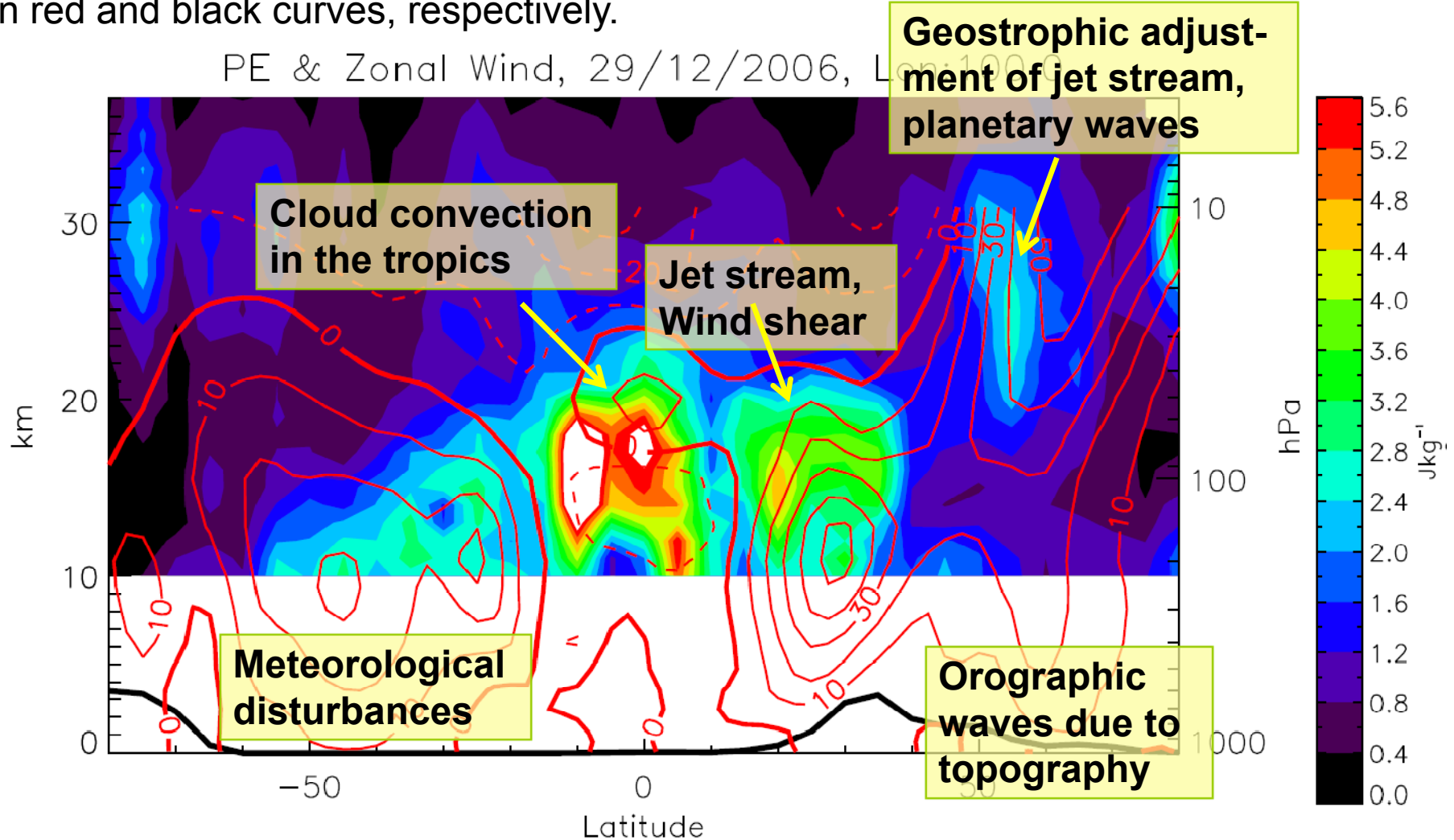
AGCM PE 140E, 1 – 7 Jan (similar wind conditions to COSMIC)

- PE from waves with periods 6hr – 1 month, $\lambda_z < 7\text{km}$, $380 < \lambda_x < 40,000\text{km}$
- Note different colour scale
- Vectors show meridional and vertical energy fluxes due to $\lambda_z < 7\text{km}$

- Comparison between the COSMIC and AGCM data indicates the relatively low PE values at 20N, which is a region that also corresponds to weaker energy flux.
- Larger PE at 40N is mostly due to subtropical jet (located equatorward of the jet), and is also distributed upward and poleward along the zonal wind contour lines.
- The polar night jet itself generates gravity waves which propagate upward and downward, as evident in (b) by the downward flux vectors on the polar side of the jet above 20 hPa.

4. Various Generation Sources of Gravity Waves

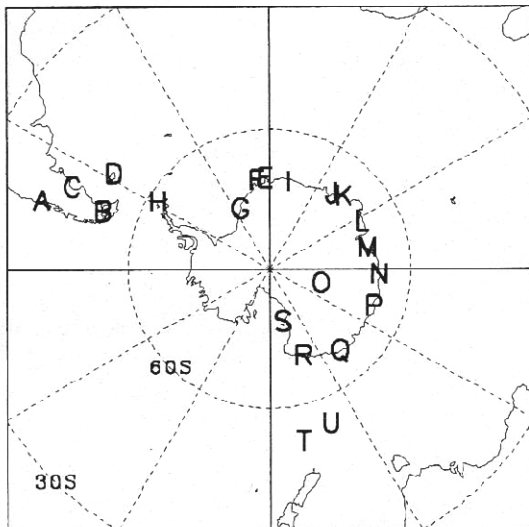
A height-latitude section of the wave potential energy (E_p) (T' with vertical wave lengths < 7 km) from the COSMIC GPS RO data in 7 days centered on **December 29, 2006 at the longitude of 140°E (130°-150°E)**. Zonal winds from NCEP and topography (elevation) at 140°E are also plotted in red and black curves, respectively.



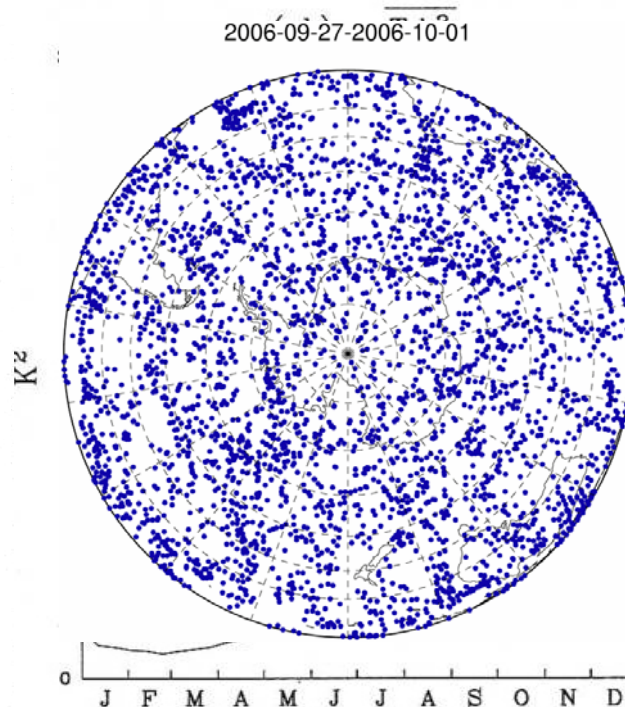
Earlier studies of gravity waves (GW) in Antarctic region

- By using routine radiosonde data at Antarctic bases, GW energy is found to be large in October-November. [Yoshiki and Sato., 2000]
- The intensity of background mean winds (polar night jet) seem to be related to a generation mechanism of GW.
- GW energy was enhanced when the polar night jet approached over the station during its dissipating phase in spring. [Yoshiki et al., 2004]
- Rantnam et al. [2004] reported enhancement of GW at around the polar vortex during the major stratospheric sudden warming in 2002 by using CHAMP GPS RO data.

(b) Southern Hemisphere

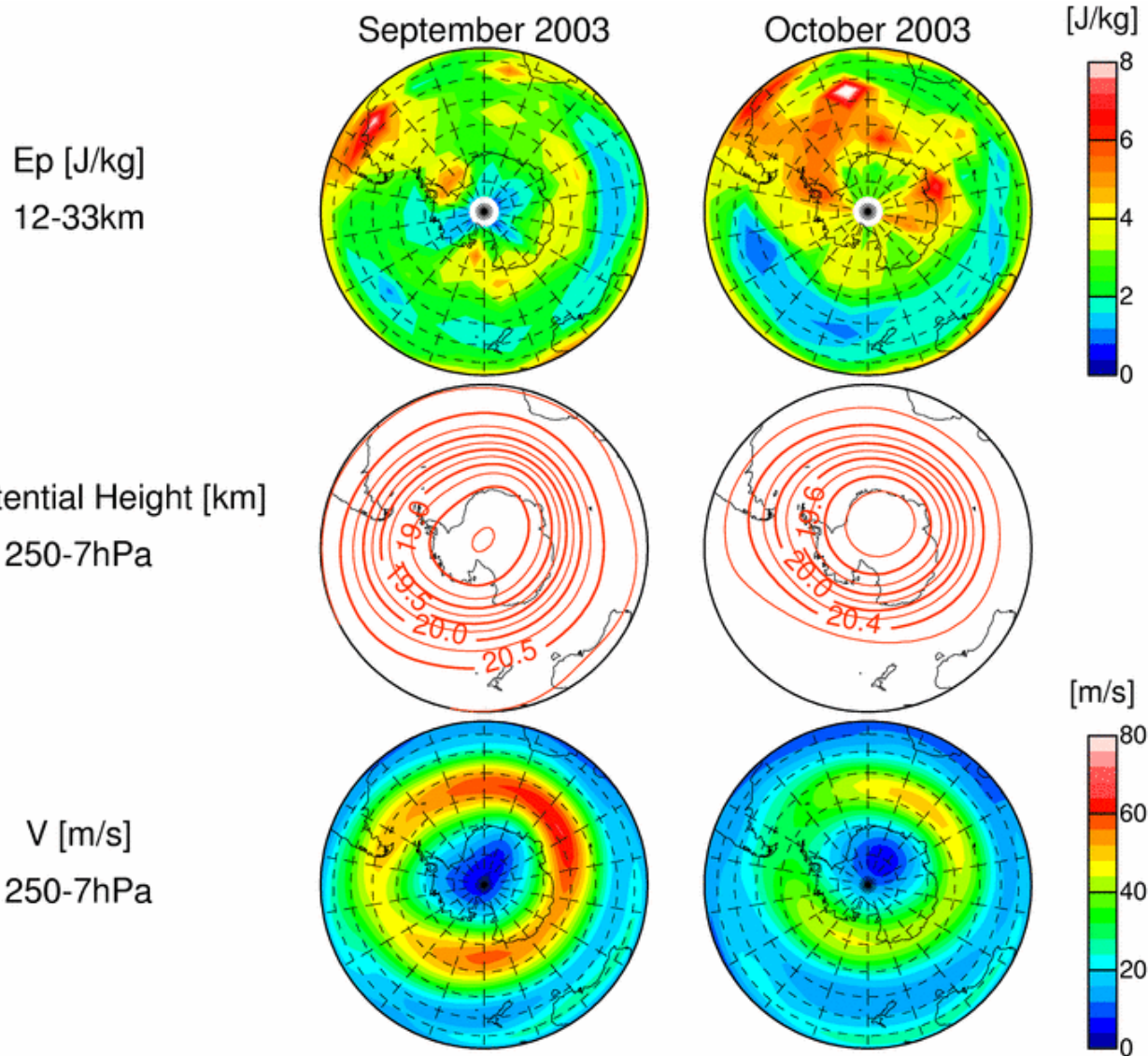


for the analysis in this study. The stations denoted by



Distribution of COSMIC
GPS RO data around
Antarctica in **5 days**
from 27 September to
1 October 2006

Horizontal distribution of Ep (12-33km), Geopotential height (250-7hPa) and Horizontal winds (250-7hPa) in September and October 2003

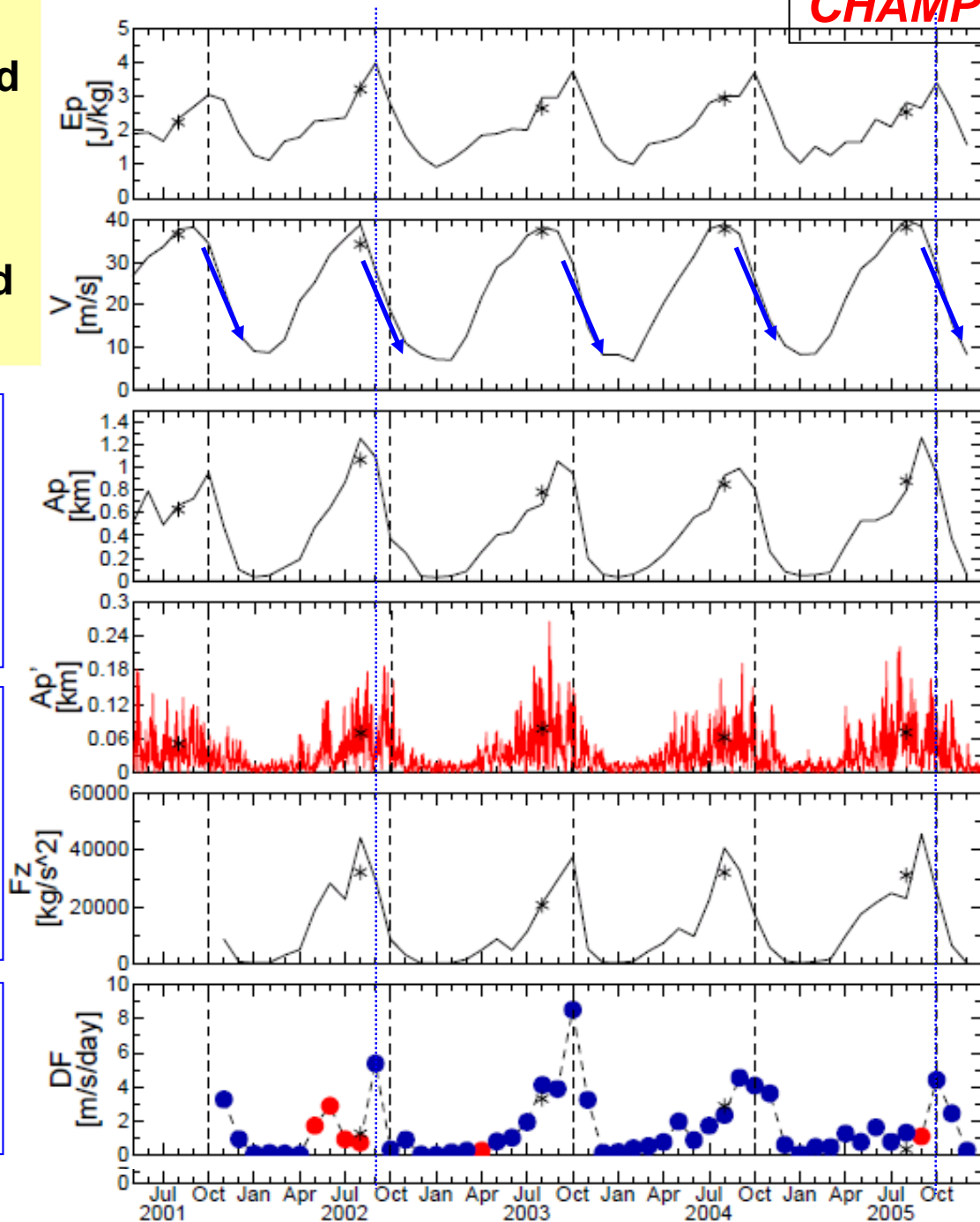


Monthly mean values of E_p (top) in the **Antarctic region** and Mean winds V , Planetary wave amplitude A_p , and its fluctuations A_p' . Vertical component of E-P flux (F_z), and E-P flux divergence (DF).

E_p gradually increases in winter (Sep-Oct), and it is largely enhanced in spring (Sep-Oct), then, it rapidly decreases.

Maximum of V occurs one month earlier than E_p peak. dV/dt coincides with E_p peak, i.e., GW are enhanced during a decay phase of polar vortex.

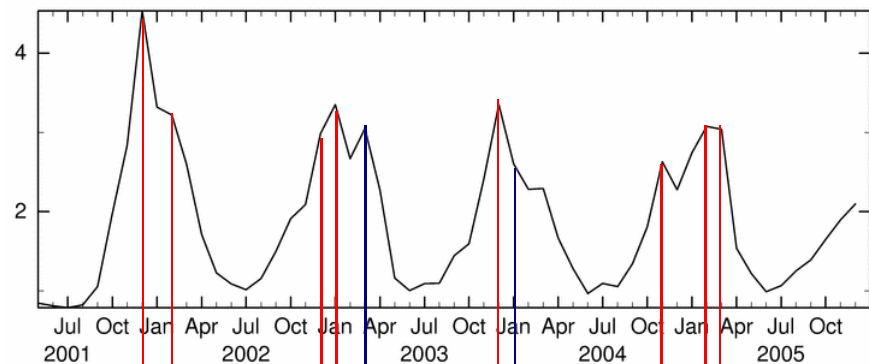
Annual cycle of F_z correlates well with E_p (and A_p as well). However, DF coincides better.



Comparison between the monthly mean Ep and E-P flux divergence in the Arctic (Left) and Antarctic (Right) regions

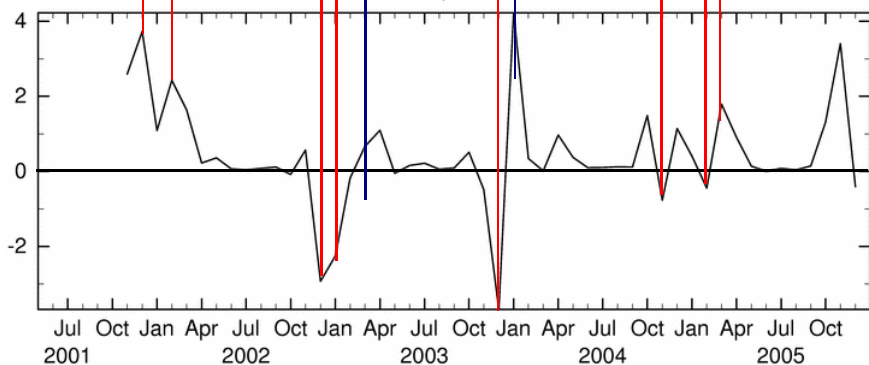
Gravity Wave Potential Energy [J/kg]

12-33km 50N-80N0-360E coe.=0.13



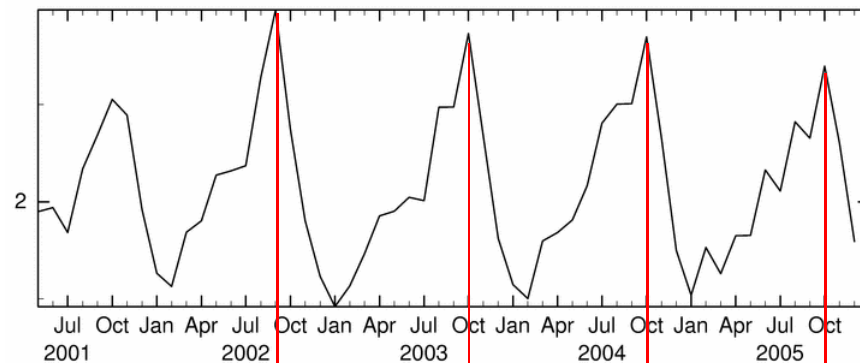
DF [m/s/day]

10hPa, 50-80N



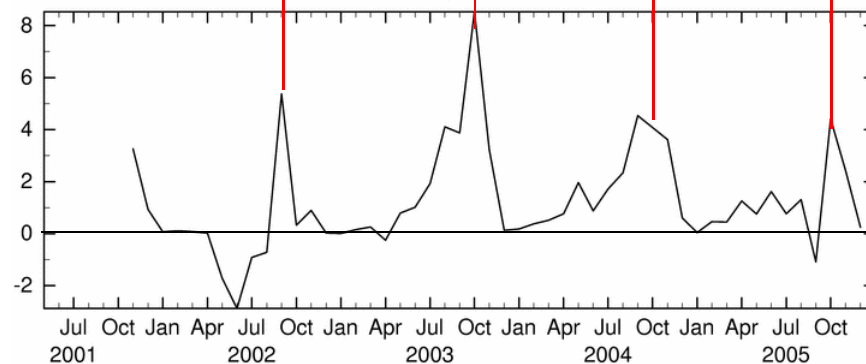
Gravity Wave Potential Energy [J/kg]

12-33km 50S-80S0-360E coe.=0.65



DF [m/s/day]

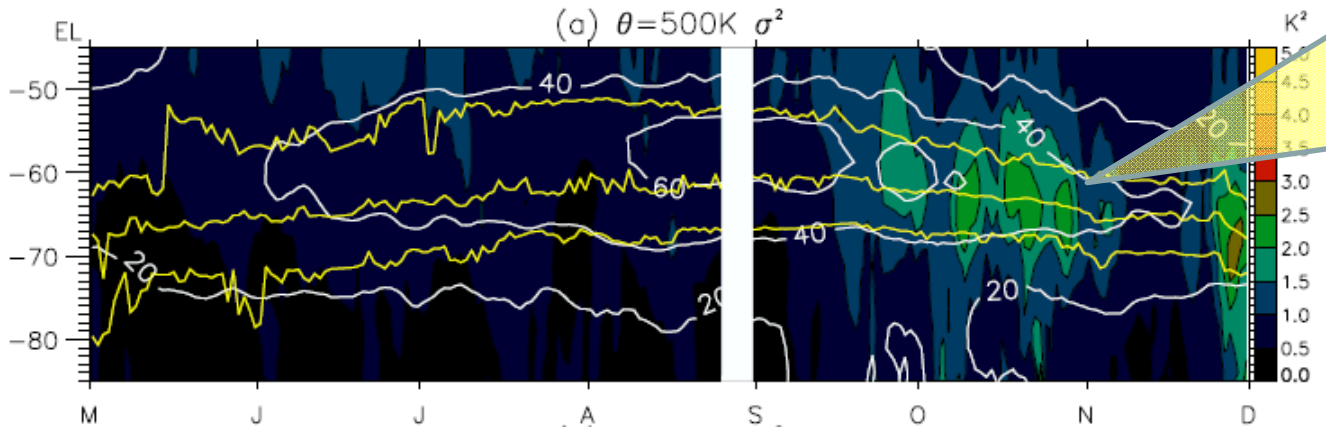
10hPa, 50-80S



A good correlation between Ep and the divergence of the E-P flux, DF, suggests that the active planetary wave generates gravity waves through planetary wave transience and/or breaking.

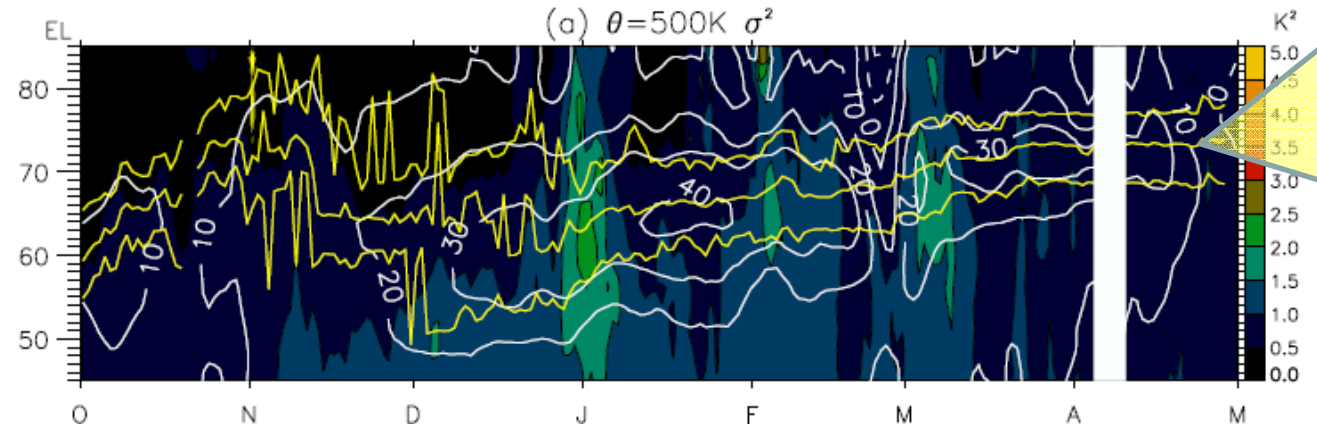
Structure of the polar vortex and wave variance (Ep) distribution

May-December 2007 in **Antarctica** at 500 K (about 19-20 km)



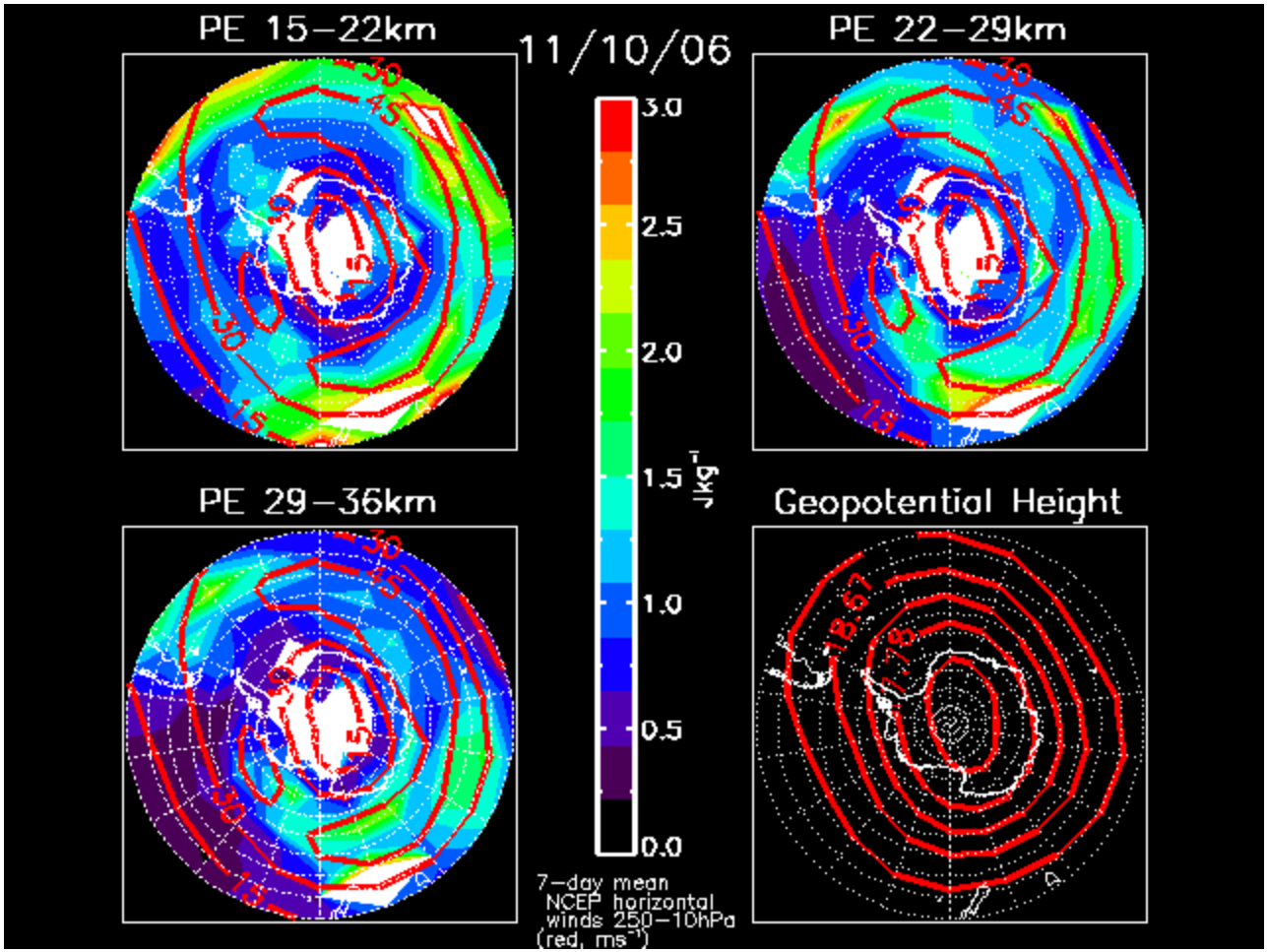
During winds decreased from 60m/s to 40 m/s in late-Sep to Oct (spring), large wave variance is observed inside the vortex boundary with symmetric distribution

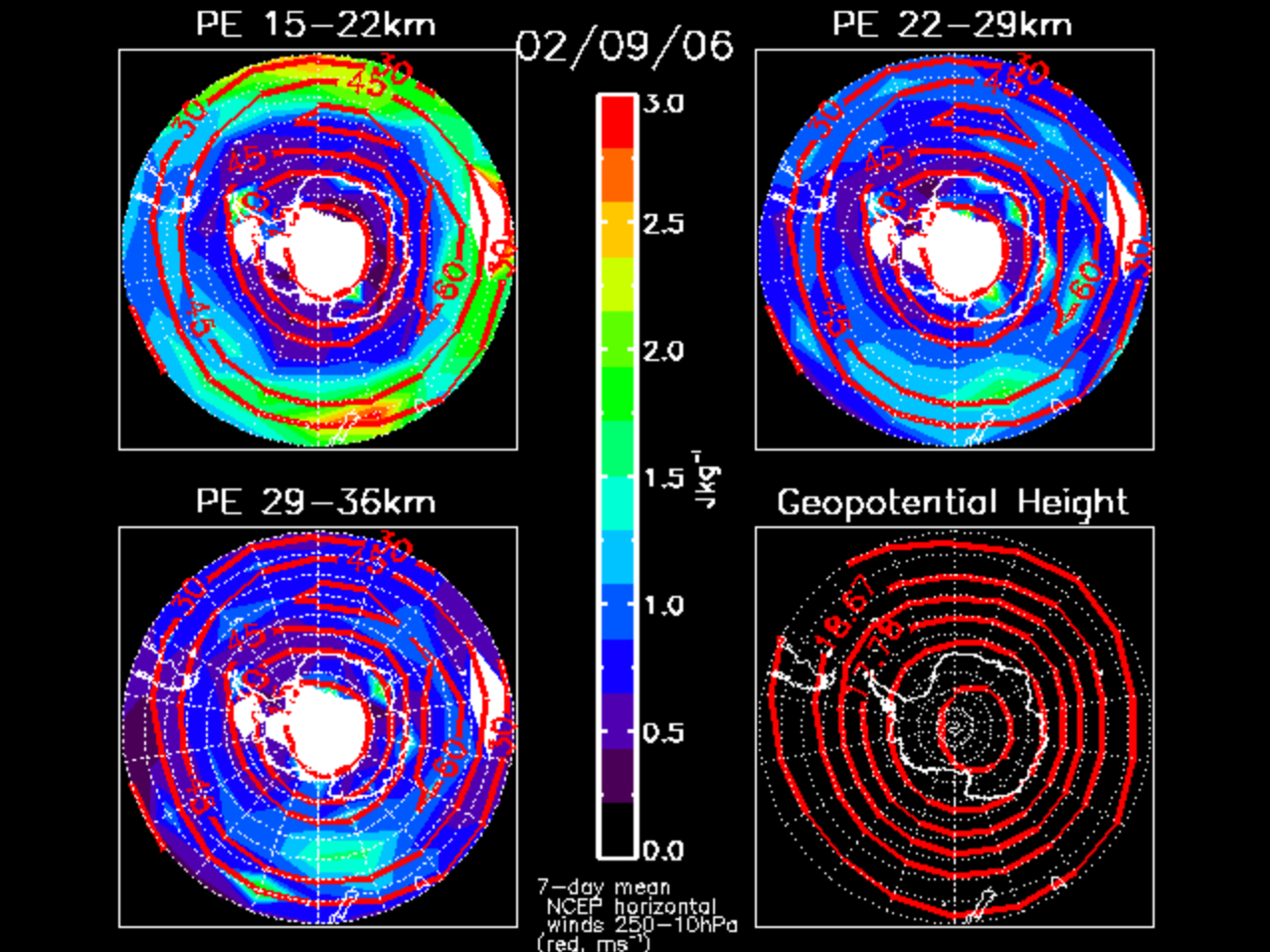
October-May 2006/7 for the **Arctic** vortex at 500 K



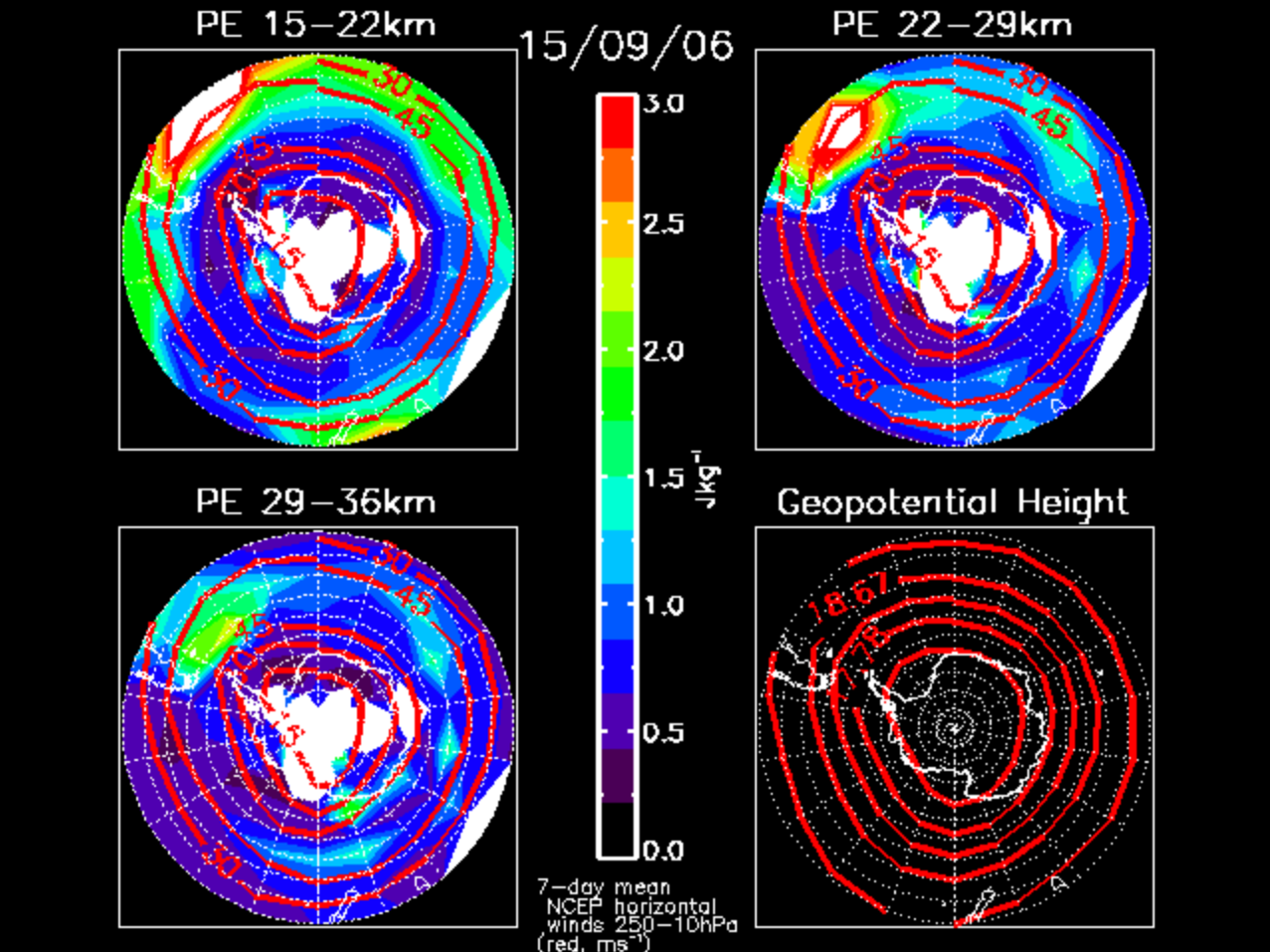
Enhancement of E_p does not occur during the vortex decay phase. But, large E_p in early Jan, Feb and March coincides with SSW (sudden stratospheric warming)

Contour: E_p , White line: 5-day smoothed UKMO zonal mean zonal winds (m/s, eastward solid),
 Yellow line: vortex edge (thick) and vortex boundary region (between the thin yellow lines).





Movie

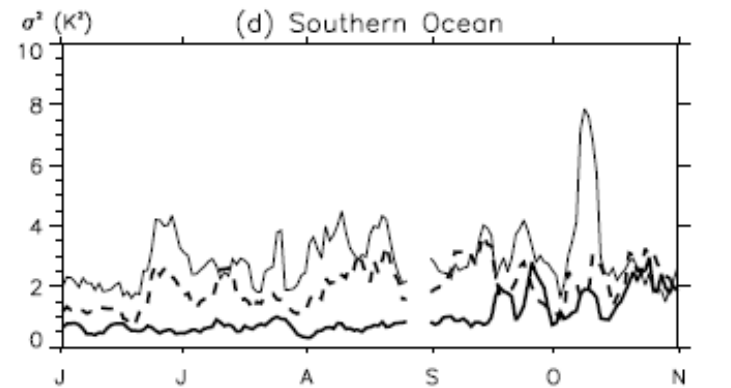
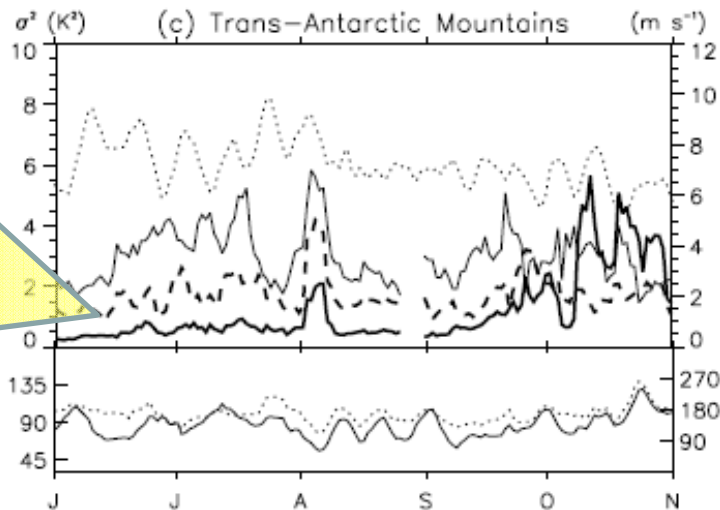
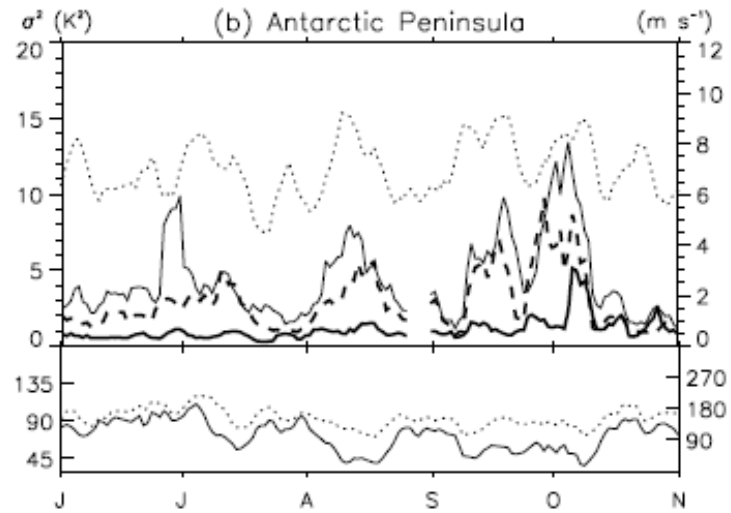
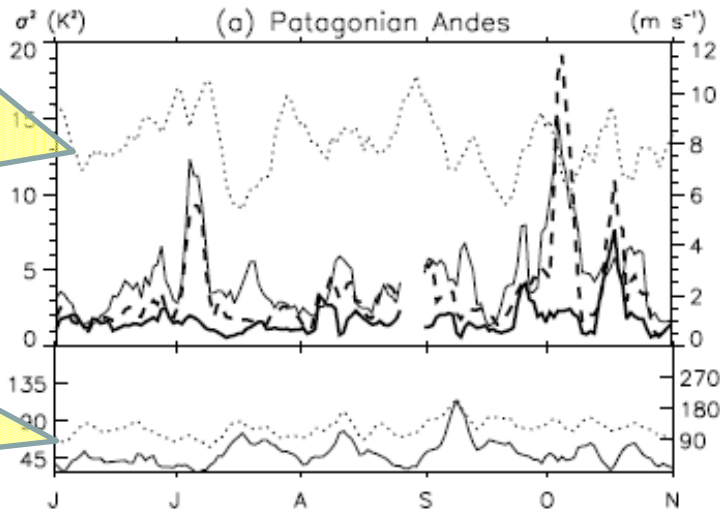


Short-term wave variability in Antarctica

Near-surface wind speed (dotted line, scale to the right)

Rotation angle of mean winds

Ep at 500 K: thick solid
800 K: dashed
1000 K: thin solid)



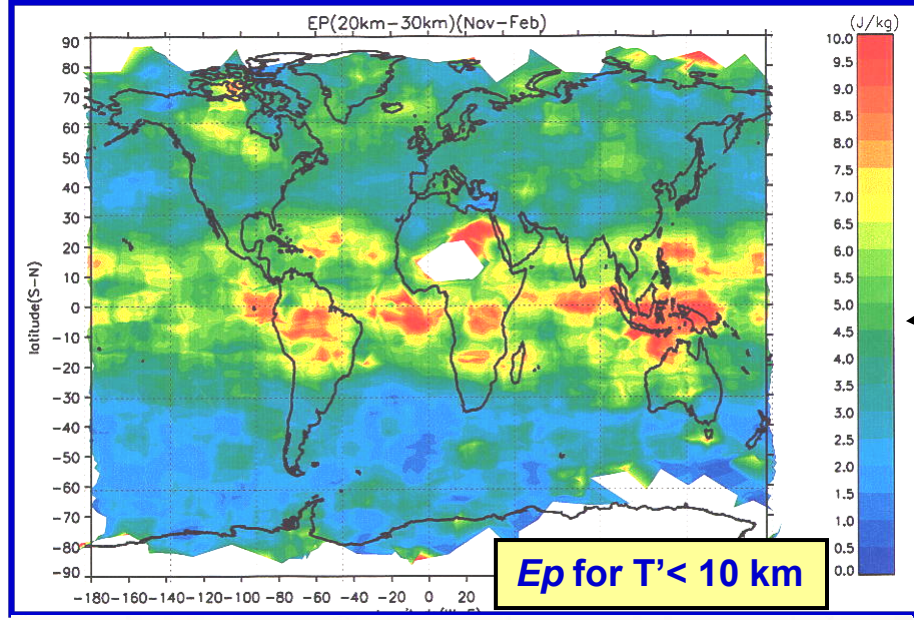
Intermittent peaks of Ep occur with 5-10 day duration, with larger values over Andes and Antarctic Peninsula than the Trans-Antarctic mountains. Orographic waves are not continuously generated, but they depend on the mean wind conditions.

Generation of gravity waves by tropical convection and effects of wave-mean flow interaction

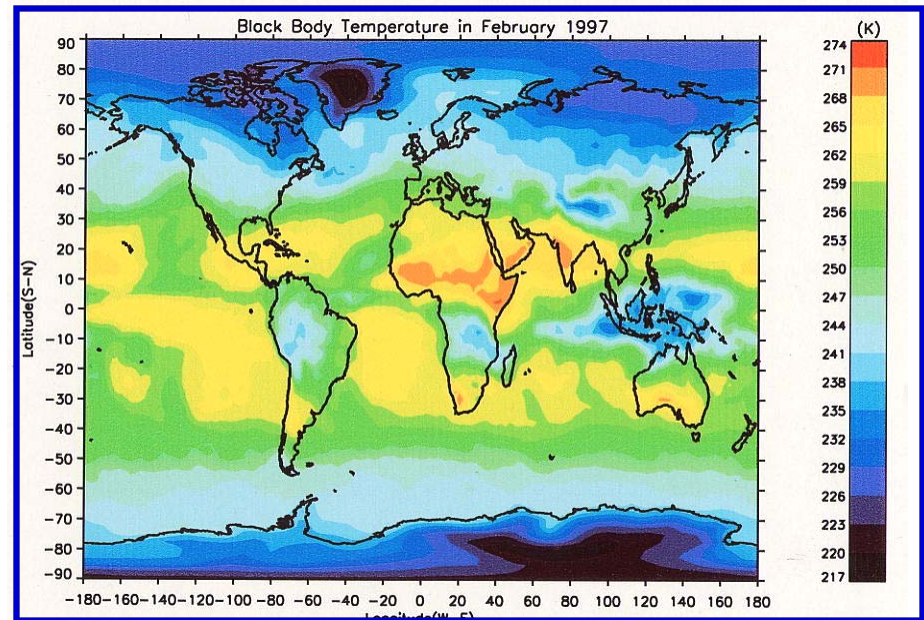
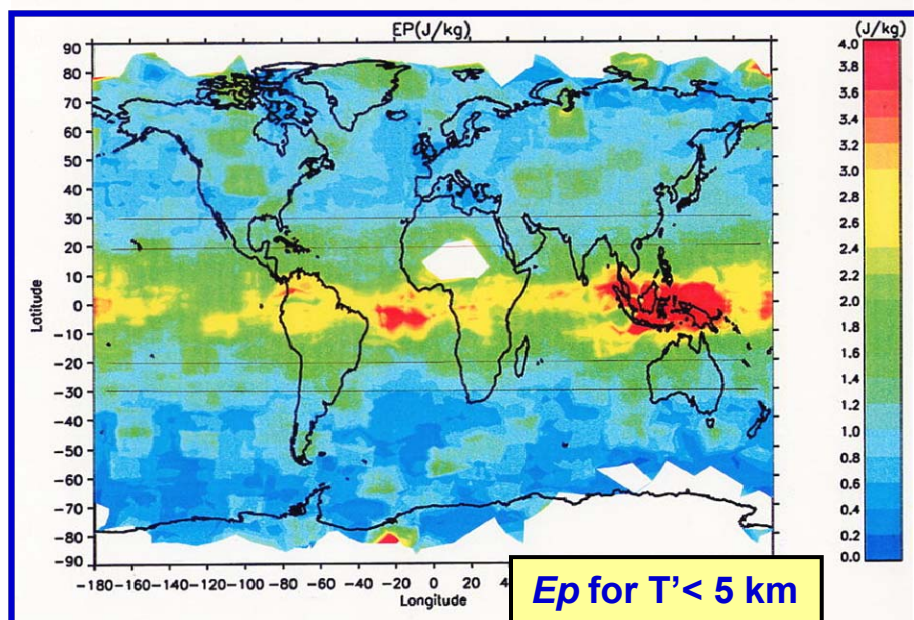


Correlation between Gravity Wave Energy (Ep) and Cloud Convection

(Left) Latitude-longitude distribution of the **wave potential energy**
 $Ep = 1/2(g/N)^2(T'/T)^2$ at 20-30 km in
 Nov-Feb from GPS/MET in 1995-1997
 (Bottom) Black body temperature (OLR)
 in Feb, 1997



Large Ep values are detected at low latitudes (25N - 25S), and they are **particularly enhanced over the regions of active convection**, i.e., Indonesia, Indian ocean, Africa and South America.

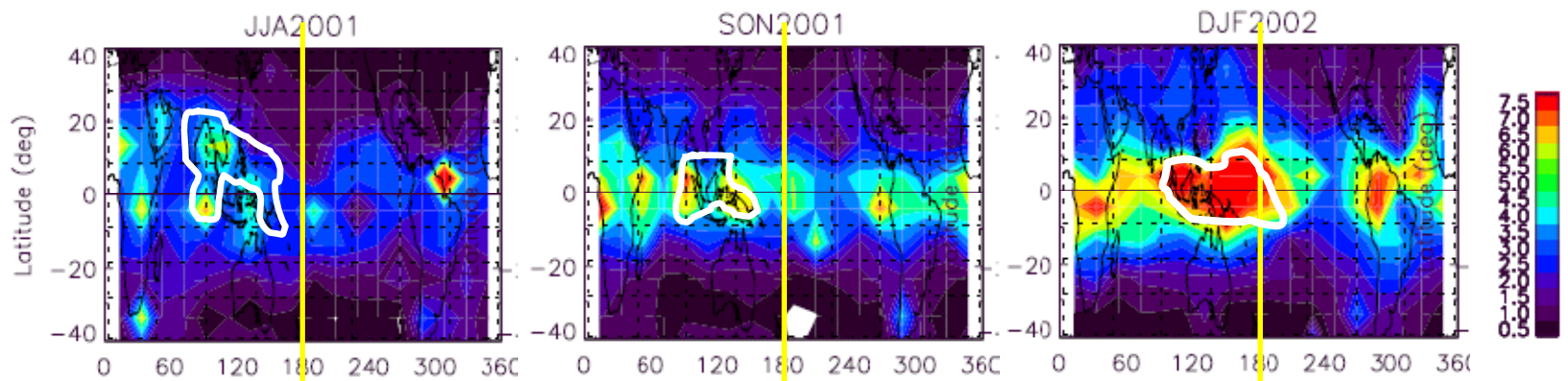


**Jun-Jul-Aug,
2001**

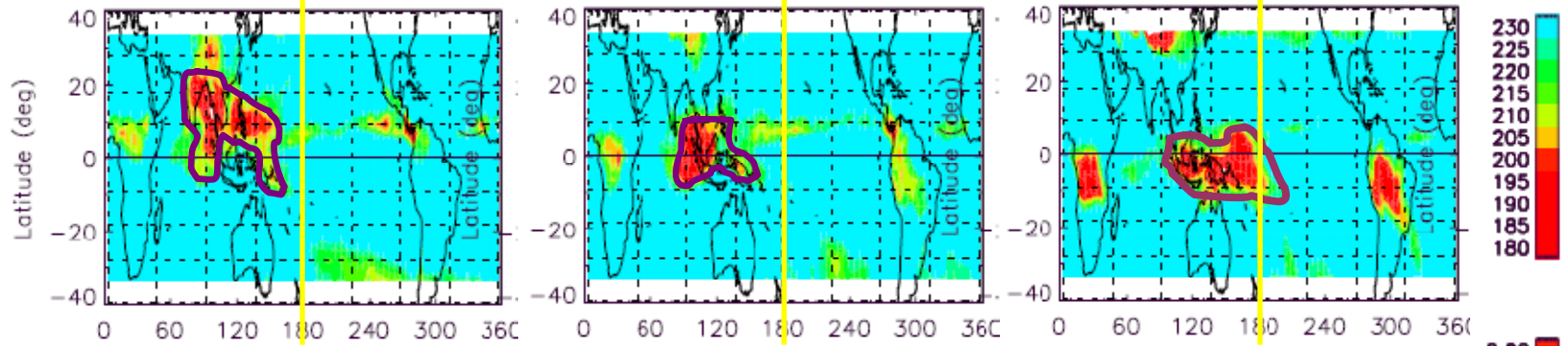
**Sep-Oct-Nov,
2001**

**Dec, 2001 –
Jan-Feb, 2002**

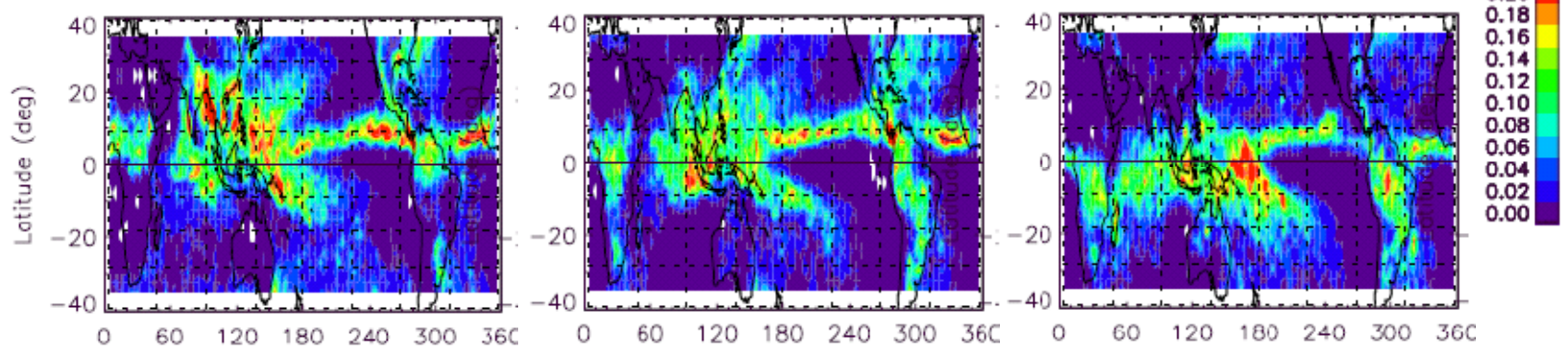
**Ep
Strato-
spheric
gravity
wave
energy**



**OLR
Cloud
top
height**

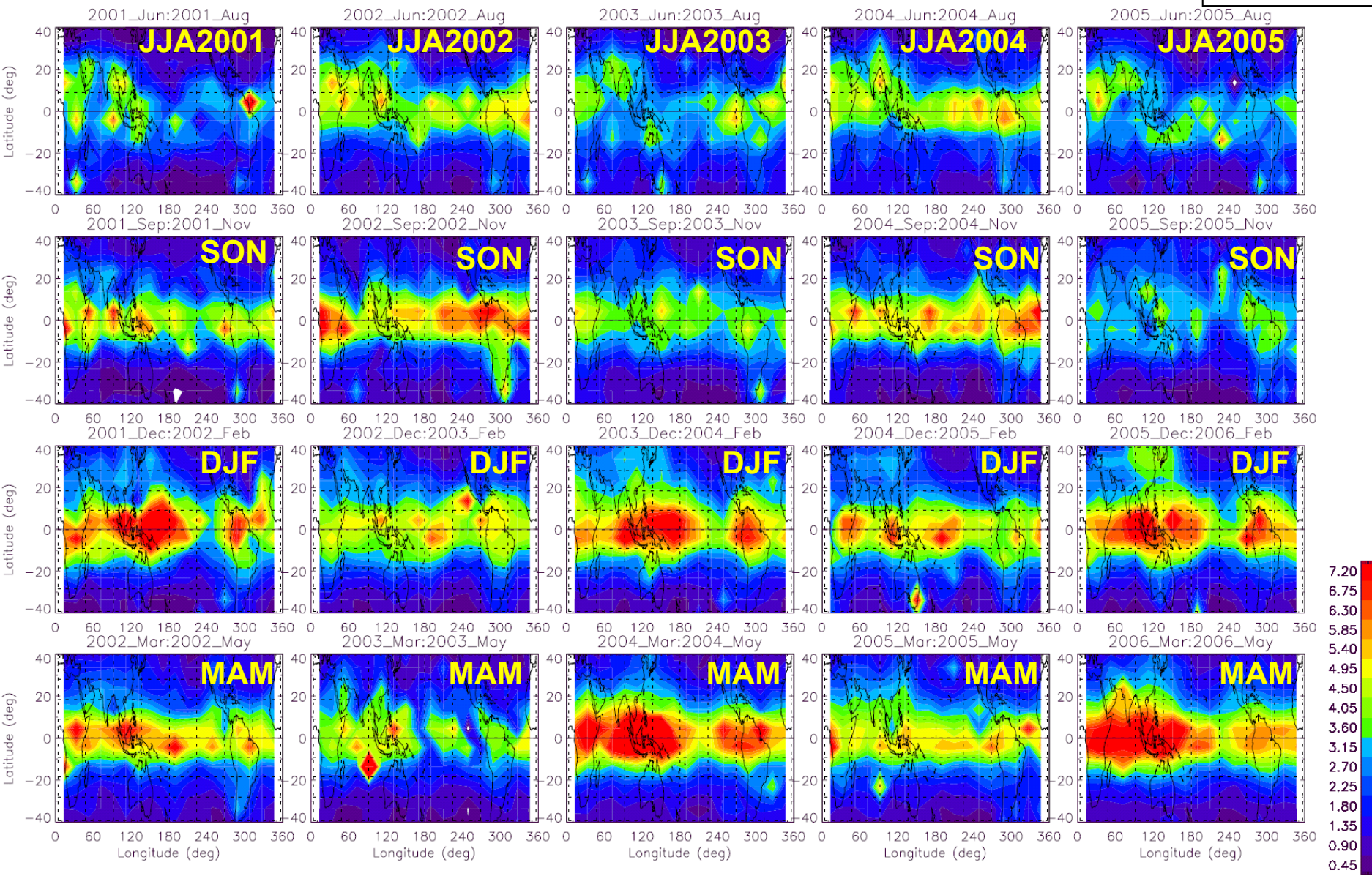


**TRMM-
PR
Convecti
ve rain
rate**



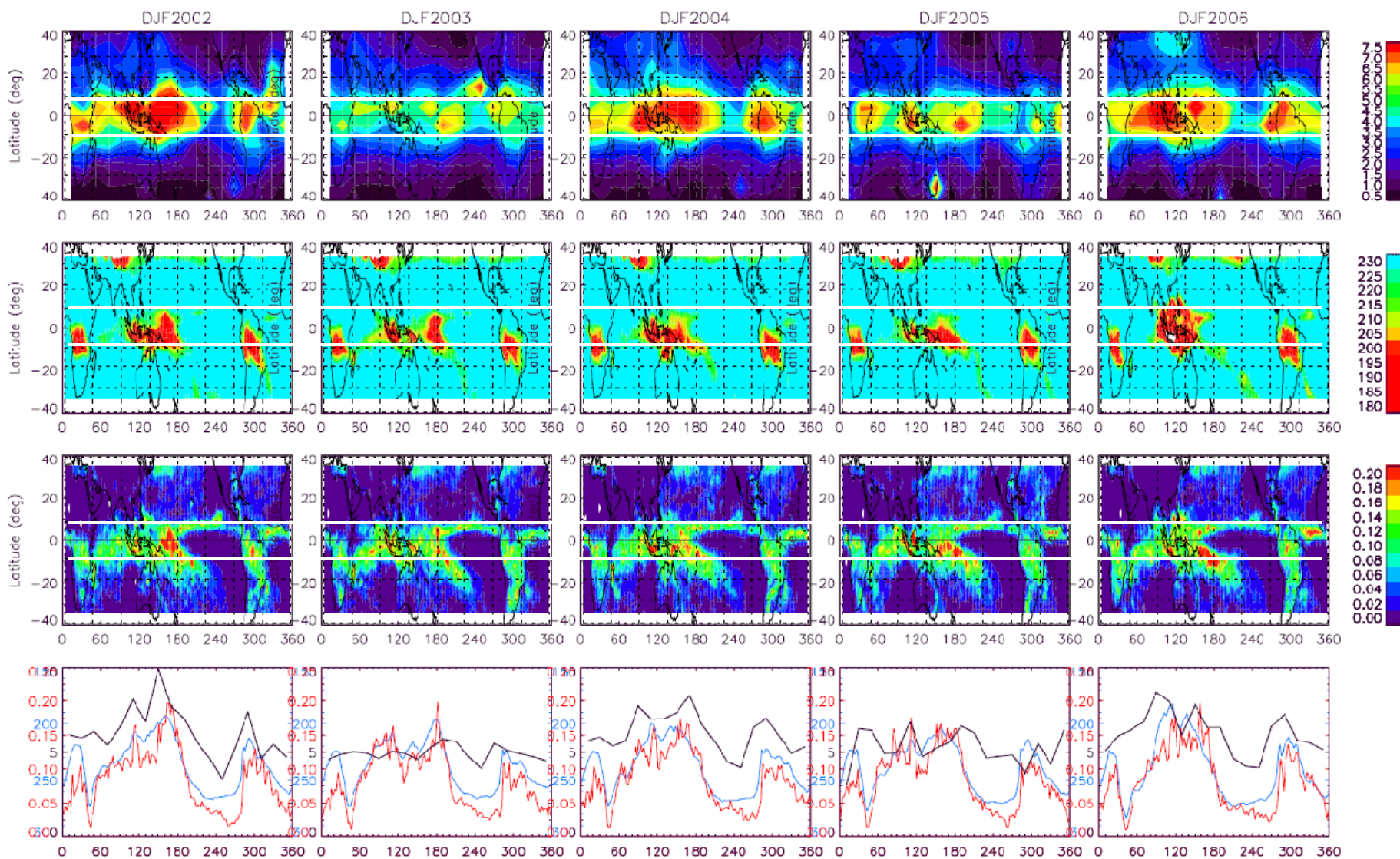
Ep with CHAMP/GPS RO in 2001–2005 19–26 km

CHAMP



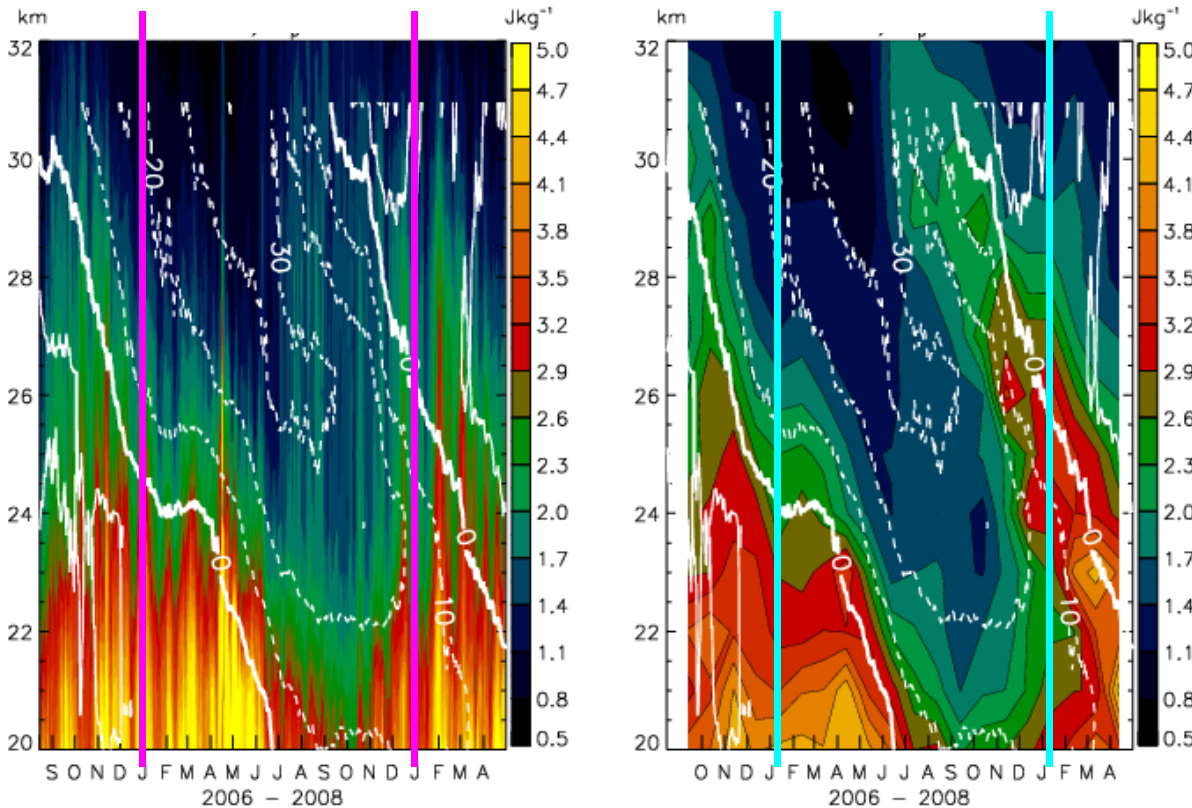
Year-to-year variations of wave energy (E_p), OLR and convective rain rate in Dec/Jan/Feb in 2001-2005

OLR, TRMM-PR, TRMM-Storm Height, E_p



Black: E_p (0-10 J/kg), Blue: OLR (300-150K), Red: Rain rate (0-0.25 mm)

Season-height section of zonal mean PE at 25.S-2.5N from Sep 2006 to Apr 2008



- QBO westward shear initially, then eastward shear after mid-2007.
- QBO removes gravity waves, especially close to the 0 m/s phase line.

LEFT:

- Grid size: $20^\circ \times 5^\circ \times 7$ days,
- 7km high-passed perturbations from individual profiles, and get PE by integrating vertically over 7km, stepping up by 1km and forward by 1 day.
- Mainly meso-scale GWs with minor MRGW and higher speed KW contributions.

RIGHT

- Grid size: $20^\circ \times 5^\circ \times$ one month
- Height independent (1km) data by assuming that all wave phases are represented at that particular height
- Slower speed KWs but still mainly consists of GWs

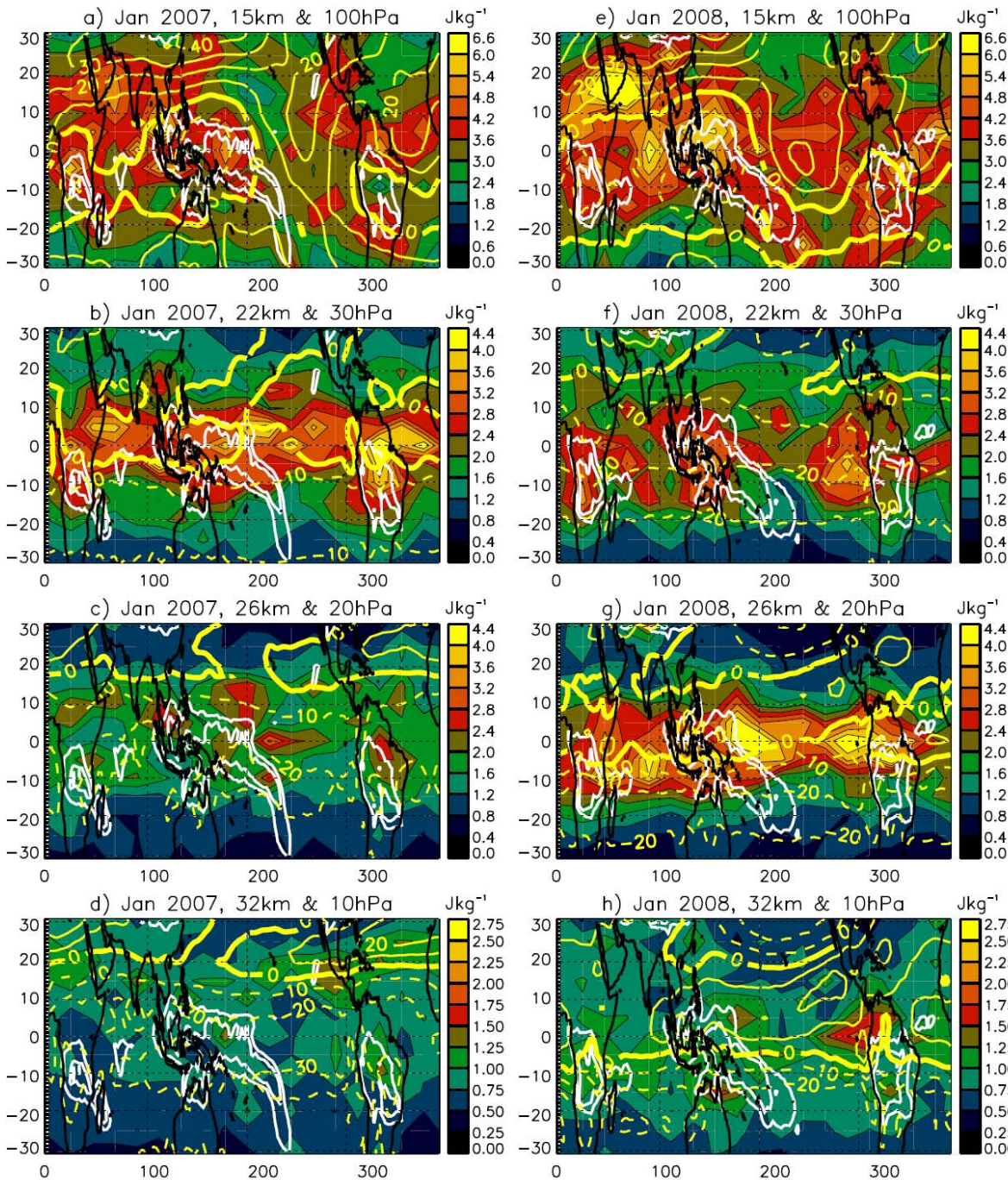
White contours: NCEP zonal mean zonal wind, units m/s, east/westward; solid dashed

PE (1 km) in Jan 2007/8

PE in January 2007 and 2008 are shown.

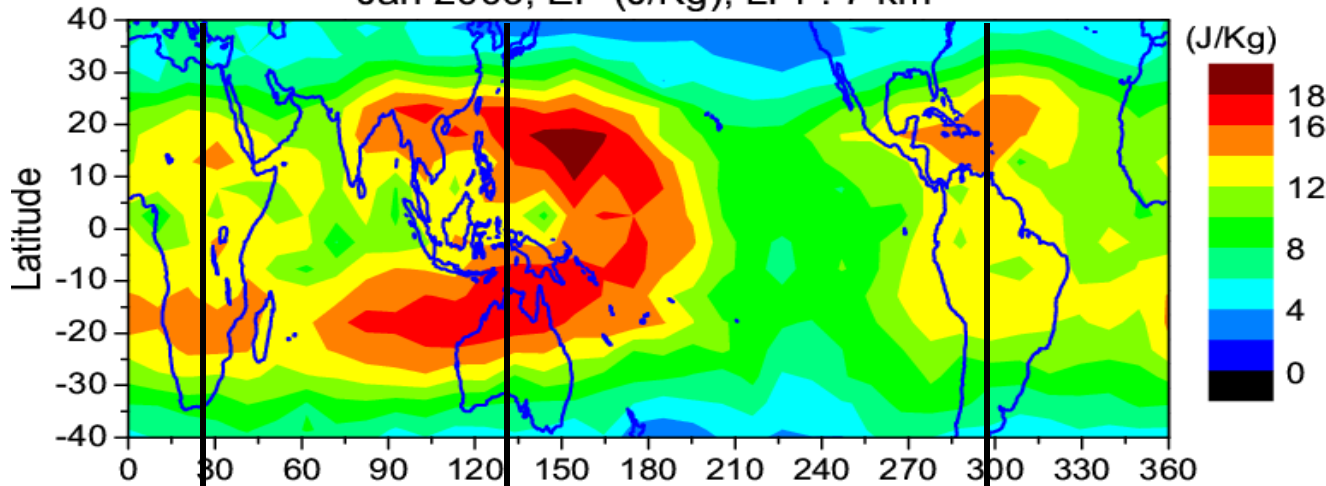
Although the convective source distribution is similar for both months, the stratospheric PE is different due to the changes in the QBO structure.

In January 2007, the QBO is in its westward shear phase with the 0 m/s line at 24 km, while one year later, the QBO is in its eastward shear phase with the 0 m/s line at 25 km.

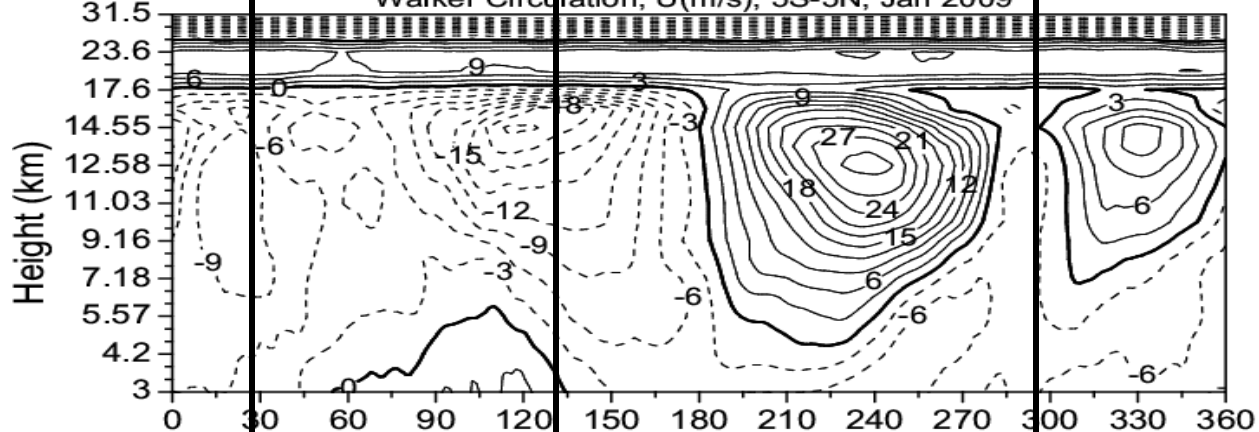


Jan 2009, EP (J/Kg), LPF: 7 km

COSMIC

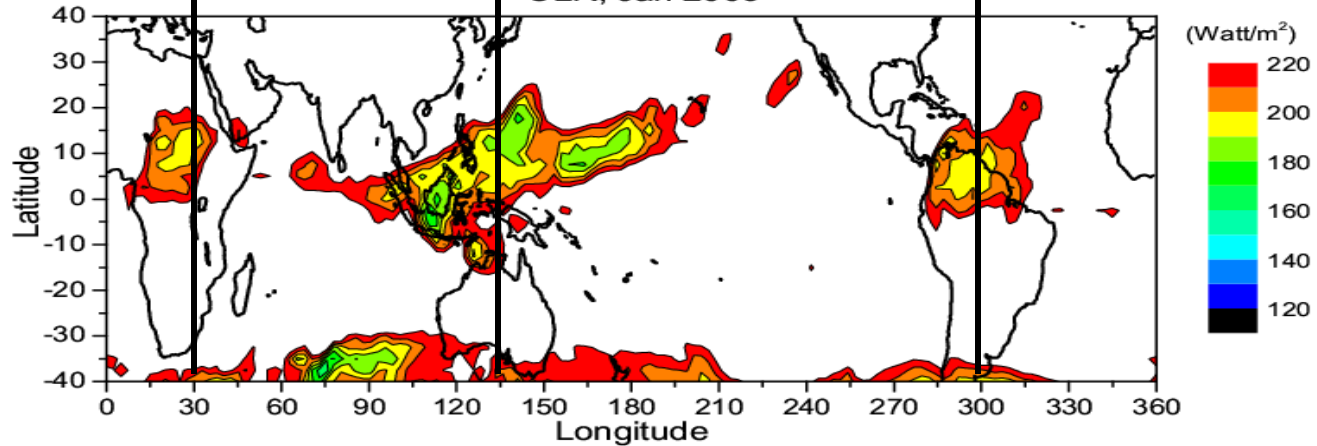


Walker Circulation, U(m/s), 5S-5N, Jan 2009



*Walker circulation
in the tropical
troposphere*

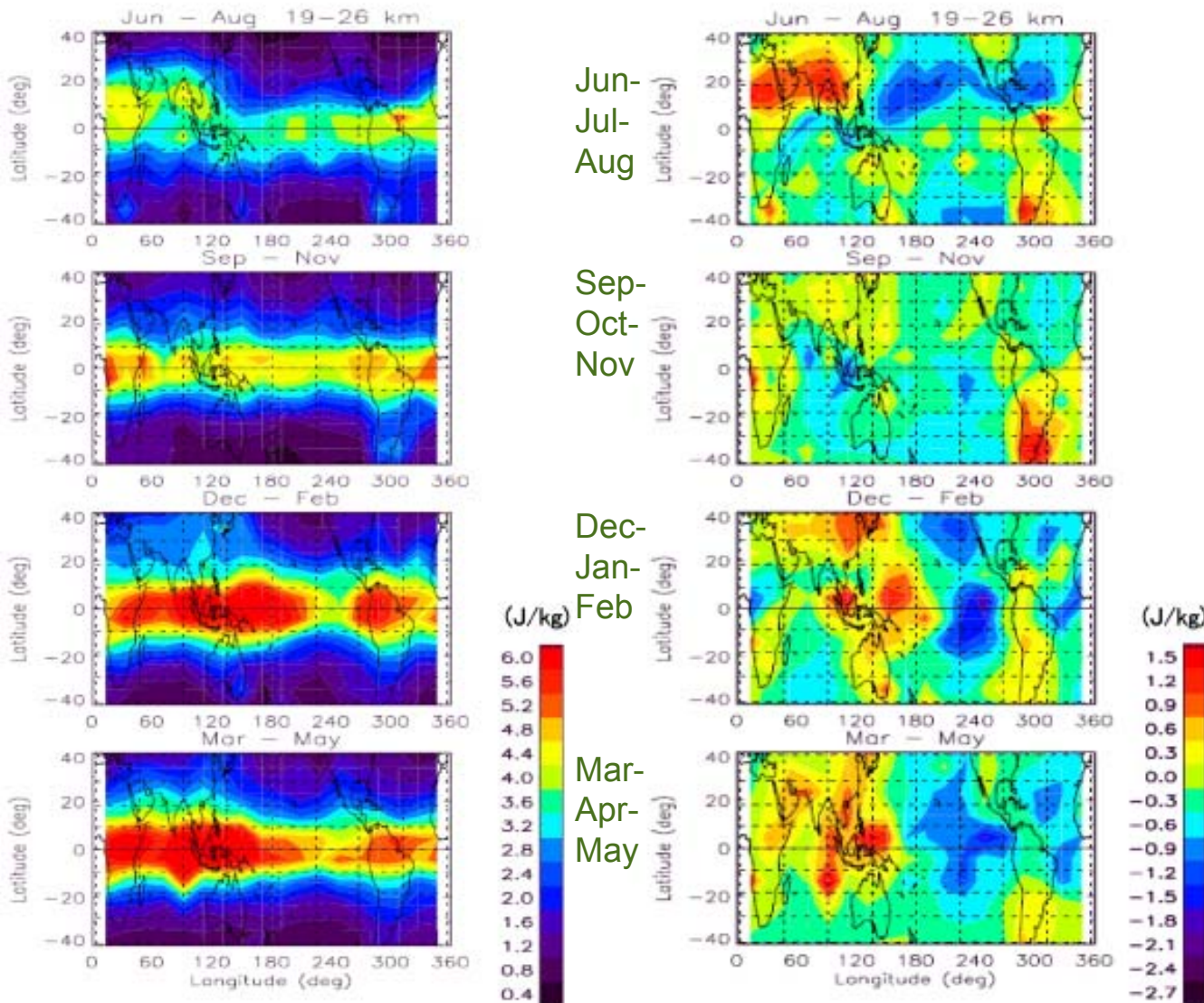
OLR, Jan 2009



(a) Longitude-latitude distribution of Ep at 19–26 km by averaging Ep in 2001–2006.

(b) In each year residual of Ep from global average in (a) is calculated, then, they are averaged for 5 years

Results in (a) indicate a climatological pattern of the temperature disturbances in the stratosphere, including Kelvin waves, GW, etc. While, (b) shows regional wave activity, esp. GW is dominant. GW energy seems to be larger over the Asian monsoon region, Indonesia-western Pacific by convection, and South America (Andes) due to orographic waves



SUMMARY

- GPS RO temperature profiles with a superior height resolution enabled us to analyse the global distribution of meso-scale temperature perturbations due to atmospheric gravity waves (GW) in the stratosphere. COSMIC data with high density have resulted in a more detailed understanding of the GW activity on shorter time intervals (5-d) than previously possible.
- Global and regional characteristics of gravity waves are studied.
 - ✓ Mid-latitudes in northern winter; GW energy in the Asian region is mostly due to the sub-tropical jet, and some additional effects by mountain waves above Canadian Rockies, Japan, and Scandinavia.
 - ✓ In the polar regions, the GW energy related to the behaviour of stratospheric polar vortex, esp. Antarctic springtime decay and SSW. Large GW energy above various mountainous regions in the polar and sub-polar regions due to orographically generated waves.
 - ✓ Tropics; Convectively generated GW is evident, showing regional and hemispheric scale changes which are related to the convective source as well as background wind conditions (QBO, Walker circulation) .



Thank you